MECHANICAL CHARACTERIZATION OF FILAMENT WOUND COMPOSITE TUBES BY INTERNAL PRESSURE TESTING

A THESIS SUBMITTED TO
THE GRADUATE SCHOOL OF NATURAL AND APPLIED SCIENCES
OF
MIDDLE EAST TECHNICAL UNIVERSITY

BY

PINAR KARPUZ

IN PARTIAL FULFILLMENT OF THE REQUIREMENTS
FOR
THE DEGREE OF MASTER OF SCIENCE
IN
METALLURGICAL AND MATERIALS ENGINNERING

MAY 2005

Approval of the Graduate School of Natural and Applied Sciences

Prof. Dr. Canan ÖZGEN
Director

I certify that this thesis satisfies all the requirements as a thesis for the degree of Master of Science.

Prof. Dr. Tayfur ÖZTÜRK
Head of Department

This is to certify that I have read this thesis and that in my opinion it is fully adequate, in scope and quality, as a thesis for the degree of Master of Science.

Prof. Dr. Alpay ANKARA
Supervisor

Examining Committee Members

Prof. Dr. Filiz SARIOĞLU	(METU, METE)	_____
Prof. Dr. Alpay ANKARA	(METU, METE)	_____
Assoc. Prof. Dr. C. Hakan GÜR	(METU, METE)	_____
Assoc. Prof. Dr. Cevdet KAYNAK	(METU, METE)	_____
Fikret ŞENEL, (M.S. in ME)	(BARIŞ IND.)	_____

I hereby declare that all information in this document has been obtained and presented in accordance with academic rules and ethical conduct. I also declare that, as required by these rules and conduct, I have fully cited and referenced all material and results that are not original to this work.

Name, Last name : Pınar KARPUZ

Signature :

ABSTRACT

MECHANICAL CHARACTERIZATION OF FILAMENT WOUND COMPOSITE TUBES BY INTERNAL PRESSURE TESTING

Karpuz, Pınar

M.S., Department of Metallurgical and Materials Engineering

Supervisor : Prof. Dr. Alpay ANKARA

May 2005, 104 pages

The aim of this study is to determine the mechanical characteristics of the filament wound composite tubes working under internal pressure loads, generating data for further investigation with a view of estimating the remaining life cycle of the tubes during service. Data is generated experimentally by measuring the mechanical behavior like strains in hoop direction, maximum hoop stresses that are formed during internal pressure loading. Results have been used to identify and generate the necessary data to be adopted in the design applications. In order to determine these parameters, internal pressure tests are done on the filament wound composite tube specimens according to ASTM D 1599-99 standard. The test tubes are manufactured by wet filament winding method, employing two different fiber types, two different fiber tension settings and five different winding angle configurations.

The internal pressure test results of these specimens are studied in order to determine the mechanical characteristics, and the effects of the production variables on the behavior of the tubes. Pressure tests revealed that the carbon fiber reinforced composite tubes exhibited a better burst performance compared to the glass fiber reinforced tubes, and the maximum burst performance is achieved at a winding angle configuration of $[\pm 54°]_3[90°]_1$. In addition, the tension setting is found not to have a significant effect on the burst performance. The burst pressure data and the final failure modes are compared with the results of the ASME Boiler and Pressure Vessel Code laminate analysis, and it was observed that there is a good agreement between the laminate analysis results and the experimental data. The stress – strain behavior in hoop direction are also studied and hoop elastic constants are determined for the tubes.

Keywords: composite, filament winding, internal pressure testing, burst pressure, hoop elastic constant.

ÖZ

FİLAMAN SARGI TEKNİĞİ İLE ÜRETİLMİŞ KOMPOZİT TÜPLERİN İÇ BASINÇ TEST YÖNTEMİYLE MEKANİK KARAKTERİZASYONU

Karpuz, Pınar
Yüksek Lisans, Metalurji ve Malzeme Mühendisliği Bölümü
Tez Yöneticisi : Prof. Dr. Alpay ANKARA

Mayıs 2005, 104 sayfa

Bu çalışmada iç basınç yükleri altında çalışan filaman sargı tekniğiyle üretilmiş kompozit tüplerin mekanik özelliklerinin belirlenmesi ve tasarım uygulamalarında ve ömür çalışmalarında kullanılmak üzere gerekli verilerin elde edilmesi amaçlanmıştır. Bu amaçla iç basınç yükleri altında malzeme içinde çevresel yönde oluşan gerinim ve gerilimler deneysel yöntemlerle ölçülmüş ve yine deneysel maksimum patlama basıncı verileriyle birlikte tasarım uygulamalarında kullanılabilecek şekilde değerlendirilmiştir. Bu özelliklerin belirlenmesi için iki farklı elyaf malzemesi, iki farklı elyaf gerilginlik değeri ve beş farklı sarım açısı konfigürasyonundan ıslak filaman sargı yöntemiyle üretilmiş kompozit tüplere ASTM D1599-99 standardının gereğince iç basınç deneyleri uygulanmıştır.

İç basınç deney sonuçları mekanik özellikleri ve üretim parametrelerinin bu özelliklere etkisini belirlemek amacıyla incelenmiştir. Bu deneyler sonucunda karbon elyafla takviye edilmiş tüplerin patlama performanslarının cam elyafla takviye edilmiş tüplere nazaran daha iyi olduğu ve maksimum patlama dayancının $[\pm 54°]_3[90°]_1$ sarım açısı konfigürasyonunda elde edildiği görülmüştür. Ekstra elyaf gerginliğinin patlama performansına önemli bir etkisi tesbit edilmemiştir. Elde edilen iç basınç patlama sonuçları "ASME Boiler and Pressure Vessel Code" lamina analiz sonuçlarıyla karşılaştırılmış ve sonuçların uyum içersinde olduğu gözlenmiştir. Çalışmada ayrıca tüplerin gerilim – gerinim davranışları incelenmiş ve çevresel yöndeki elastik sabitleri de hesaplanmıştır.

Anahtar Kelimeler: kompozit, filaman sargı, iç basınç deneyi, patlama basıncı, çevresel elastik sabit.

To My Family

ACKNOWLEDGMENTS

I would like to thank Prof. Dr. Alpay ANKARA for his guidance, encouragement, insight, advice and criticism throughout the research.

I also want to express my thanks to the examining committee members for their invaluable contributions to this thesis.

I am deeply thankful to mom and dad, whose emotional strength, free-flowing love and caring concern have helped shape my maturation. Without their patience and support, the research period would have been a complete disaster.

I want to thank all the BARIŞ Elektrik Endüstrisi A.Ş. staff for their support. But I want to express my special thanks to Aybars GEDİZ, Fikret ŞENEL and Gökhan GÜVEN for their continuous concern, help and support; and their friendly and humorous, but very kind attitude towards me all throughout this work. In addition, the technical assistance and efforts of Hasan DEVREZ are greatly acknowledged.

Finally, I want to thank all my friends, especially to Ahmet Semih SUNKAR, for their moral support in every occasion, thus making this study easier and more bearable for me.

This study was supported by METU Scientific Research Project Funds; Grant No: BAP-2004-03-08-05.

TABLE OF CONTENTS

LIST OF TABLES

TABLES

LIST OF FIGURES

FIGURES

CHAPTER I

INTRODUCTION

Many of the modern industrial applications and technologies require materials with superior properties that cannot be met by conventional monolithic materials, such as metal alloys, ceramics, and polymers. Considering the principle of the combined action, better properties can be obtained by combination of two or more distinct materials. Accordingly, material property combinations have been, and yet being extended by the development of the composite, which is a multiphase material that exhibits a proportion of the properties of the forming phases so that a better combination of properties is obtained. Composites may have different properties that its constituents do not posses, such as impact resistance being high for HPPE composites.

Composite materials have several advantages over traditional engineering materials, which make them attractive for many industrial applications. Composite materials have superior mechanical properties like high specific stiffness, high specific strength, high fatigue strength, and good impact properties. They can easily act as "smart" materials, that is, they can provide in-service monitoring or online process monitoring with the help of embedded sensors. Unlike most metallic materials, they may offer high corrosion and chemical resistance. Besides, composite materials provide good dimensional stability and design flexibility, they are appropriate for near-net-shape processing, which eliminate several machining operations and thus reduces process cycle time and cost. Although composites could offer many beneficial properties, they suffer from the following disadvantages: compared to most of the traditional engineering materials, material cost of the composite materials is high, their high-volume production methods limit the widespread use of composites. A problem with polymer matrix composites is that they absorb serious

amounts of moisture, which, affects the mechanical properties and dimensional stability of the components. The temperature resistance and solvent resistance depend strongly on the matrix material.

Composite structures are employed in a wide range of industrial applications; transportation, aerospace, automotive, construction, marine, military, electronics, sports, civil engineering, etc. S.K. Mazumdar [1] reported the levels of composite shipments up to 545 million kg for transportation industries, and 340 million kg for construction industries in the USA for the year 2000. Also, composites have a great share in the high technology industries such as aerospace, defense, electronics, etc, up to shipment levels of 180 million kg.

Composites are also used in several design applications. Composites can be designed for different types of (tensile, compressive, impact, internal, torsion, and possible combinations of these) loading. For design purposes, it is vital to clarify the mechanical responses of composites to the mentioned loading types. As a result, studies are and being carried out to determine the mechanical behavior of composite structures under different loading conditions.

1.1 Objective of the Study

The objective of the study is to assess the mechanical behavior of the filament wound composite tubes working under internal pressure by experimental techniques to develop a database for design of filament wound pressure vessels and determination of their useful life cycle. To find these,

- Maximum hoop stresses formed during loading,
- Strains in hoop direction,
- Elastic constants in hoop direction,

will be determined, and thus the necessary data of to be used in the design applications will be generated and identified.

To obtain this data, a proper gripping system, an internal liner and end reinforcements are designed for the test tubes, and the test tubes are manufactured by wet filament winding method. Internal pressure tests are applied on the test tubes according to ASTM D 1599-99 standard, and the test results are evaluated and compared with the data in literature.

Chapter 2 of the thesis will cover the theory of the composites; definitions, classifications, materials used, production techniques and tests performed to identify the mechanical properties and a brief literature review. Chapter 3 is on the experimental work; test design, testing procedure, specimen geometry, materials used and tube manufacturing. Chapter 4 describes the experimental results; burst test and strain gauge data and their evaluation so that mechanical parameters are identified and presented. Chapter 5 discusses the experimental results considering the production variables; compare these results with the results obtained by different mechanical testing methods and laminate analysis methods in literature. Chapter 6 concludes the study and gives possible future work.

CHAPTER II

THEORY AND LITERATURE REVIEW

2.1 Composites

Nature is full of examples where the idea of composites is present. The coconut palm leaf, for example, is nothing but a cantilever using the concept of fiber reinforcement. Wood is a fibrous composite: cellulose fibers in a lignin matrix. The animal body is a composite of bone and tissue, where a bone itself is a natural composite that supports the weight of various members of body. It consists of short and soft collagen fibers embedded in a mineral matrix called apatite [2].

Strictly speaking, the idea of composite materials is not a new one. Ever since it was recognized that combinations of different materials often resulted in superior products, materials have been combined to produce composites. Mud bricks reinforced with straw were known to have been made hundreds of years B.C., as were laminated woods. Early history reports Mongol bows made from cattle tendons, wood and silk bonded together with adhesives. Other examples include Japanese ceremonial swords and Damascus gun barrels fabricated from iron and steel laminates. In recent history, World War II can be considered to be a milestone for the further development of composite technology. Nevertheless, the origin of a distinct discipline of composite materials can safely be marked as the beginning of 1960s. Since the early 1960s, there has been an ever increasing demand for materials ever stiffer and stronger yet lighter in fields as diverse as space, aeronautics, energy, civil construction, etc. The demands made on materials for better overall performance are so great and diverse that no one material is able to satisfy them. This naturally led to a resurgence of the ancient concept of combining different materials in an integral-composite material to satisfy the user requirements. Such composite material systems

result in performance unattainable by the individual constituents and they offer a great advantage of a flexible design [2,3].

At present, there is no universally accepted definition of the term "composite material". One definition might be "any material that consists of two or more identifiable constituents" [3]. Such a definition could include almost everything (excluding the single-phase, homogeneous materials); rocks, minerals, wood, animal bones, etc. Even a metal can be considered to be a composite of many grains. In order to avoid contra-version, an operational definition for composite should be given, and that definition is as follows: A substance consisting of two or more materials, insoluble in one another, which are combined to form a useful engineering material possessing certain properties not possessed by the constituents, is called a "composite material" [4].

Many composite materials are composed of just two phases; one is termed the matrix, which is continuous and surrounds the other phase, often called the dispersed phase or the reinforcement. The properties of composites are a function of the properties of the constituent phases, their relative amounts, and the geometry (shape of the particles, particle size, distribution and orientation) of the dispersed phase.

2.1.1 Classification of Composites

The composites may be classified according to their reinforcement types: particle reinforced composites and fiber reinforced composites. But more commonly, the classification is based on the matrix type: metal matrix composites (MMCs), ceramic matrix composites (CMCs) and polymer matrix composites (PMCs).

2.1.1.1 Metal Matrix Composites

The MMCs are materials consisting of metal alloys reinforced with continuous fibers, particulates or whiskers. The addition of these reinforcements gives MMCs

superior mechanical properties and unique physical characteristics. The two most commonly used metal matrices are based on Aluminum and Titanium which both have comparatively low specific gravities. Also, Beryllium, Magnesium, Nickel and Cobalt based super alloys are can be used as matrix materials regarding the needs and service conditions of the application. As reinforcement, generally SiC particles, Boron and Al_2O_3 fibers, and Borsic (Boron fibers coated with SiC) and TiB_2 coated carbon fibers are employed. Because of their ability to provide the needed strength at the lowest weight and least volume, MMCs are attractive for many structural and nonstructural applications.

2.1.1.2 Ceramic Matrix Composites

CMCs in which ceramic or glass matrices are reinforced with continuous fibers, whiskers, or particulates, mainly SiC and Si_3N_4, are rising as a type of advanced engineering structural materials. Ceramics have very attractive properties for many applications; high strength and stiffness at high temperatures, low density and chemical inertness. But the one serious disadvantage of this class of material is that their susceptibility to impact damage and catastrophic failure in presence of flaws. CMCs has been to toughen the ceramic matrices by incorporating reinforcements in them and thus obtain the attractive high temperature properties with drastically decreasing the risk of sudden catastrophic failures.

2.1.1.3 Polymer Matrix Composites (PMCs)

The thesis is on PMCs. Therefore major emphasis will be given to this topic.

PMCs consist of a polymer matrix, either thermoset or thermoplastic, and fibers or other materials with sufficient aspect ratio as the reinforcing medium, which, in general, is glass, Carbon, Boron and Kevlar. The low weight of the matrix material is accompanied by the attractive mechanical properties of the reinforcement. As a result, a composite material with quite high specific mechanical properties is

obtained, accompanied with low cost and ease of fabrication, which is widely employed in several application areas.

2.1.1.3.1 Matrix Materials

In polymer matrix composites, as in all composite materials, the matrix serves to transfer stresses between the fibers, holds the reinforcement phase in place and protects the surface of the fibers from mechanical abrasion. It has a minor role in tensile load carrying capacity of the composite structure.

Polymers are particularly attractive as matrix materials due to their relatively easy processibility, low density and good mechanical and dielectric properties. They are divided into two broad categories: thermoplastics and thermosets. The thermoplastic polymers can be heat-softened, melted and reshaped many times. In a thermoset polymer, however, the cross links that form a rigid network of molecules cannot be broken; thus the polymer cannot be melted or reshaped by application of heat and pressure.

When combined with reinforcements, thermoplastic polymers offer unique advantages. The most important advantages are lower cost of manufacturing, accompanied with high impact strength and high fracture resistance. These attractive mechanical properties result in a very good damage tolerant behavior in the composite. Generally, compared to thermoset polymers, thermoplastics have higher strains to failure, which shall provide better resistance to many mechanical damage types, like matrix microcracking. The most common thermoplastic resins employed in composite manufacturing and their common characteristics are as follows:

- Nylon, which has high toughness and impact resistance,
- Polyetheretherketone (PEEK), with excellent chemical and wear resistance,
- Polypropylene (PP), with high specific strength, low cost, very good chemical resistance and ductility,

- Polyphenylene sulphide (PPS), with excellent balance in strength and high temperature resistance at low cost,
- Polyimides (PAI), that have relatively high service temperature range.

Traditionally, thermoset polymers are employed in fiber reinforced composites. They are an important source of properties, superior mechanical characteristics, and better handling properties compared to thermoplastic resin systems. The most common thermoset resins employed in the composite manufacturing and their common characteristics are as follows:

- Unsaturated polyesters, with attractive mechanical, chemical and electrical properties accompanied with dimensional stability, cost and ease of processing and fast curing,
- Epoxies, with superior mechanical and electrical properties, resistance to corrosive environments, good performance at elevated temperatures,
- Vinyl esters, which combine the superior mechanical properties of epoxy resins with the handling advantages of the unsaturated polyester resins,
- Phenolics, with high performance characteristics like high temperature, chemical and creep resistance,
- Polyurethans, with good impact resistance, and
- Bismaleimides (BMI), with high temperature resistance.

The mechanical properties of polymeric resin systems employed as matrix materials are given in Table 2.1.

Table 2.1 Mechanical properties of resins [5].

Resin Type	Density (Mg/m3)	Modulus (GPa)	Strength (MPa)
THERMOPLASTIC			
Nylon			
PEEK	1.26 – 1.32	3.2	93
PP	0.9	1.1 – 1.6	31 – 42
PPS	1.36	3.3	84
PAI	1.4	3.7 – 4.8	93 – 147
THERMOSET			
Polyester	1.1 – 1.23	3.1 – 4.6	50 – 75
Epoxy	1.1 – 1.2	2.6 – 3.8	60 – 85
Vinyl Ester	1.12 – 1.13	3.1 – 3.3	60 – 90
Phenolic	1.0 – 1.25	3.0 – 4.0	60 – 80
Polyurethan	1.2	0.7	30 – 40
Bismaleimides	1.2 – 1.32	3.2 – 5.0	48 – 110

2.1.1.3.2 Reinforcement Materials

Reinforcements for PMCs can be fibers, particles or whiskers. Each has its own unique application, although fibers are the most common, and have the greatest influence on properties. Fibers are the materials with very high aspect ratios; i.e. they have one very long dimension compared to the others. They have significantly more strength in the long direction than the other directions.

The most common fiber reinforcements for PMCs and their common characteristics are as follows:

- Glass fibers with different special characteristics:
    - E glass, with high electrical insulating properties,
    - S glass, with high strength, heat resistance and modulus,
    - S2 glass, with similar properties to S glass, but of lower cost,
    - C glass, with high chemical corrosion resistance,
    - A glass, with high alkali content and thus excellent chemical resistance but lower electrical properties,
    - D glass, with excellent electrical properties, but lower mechanical properties.
- C (graphite) fiber, with very high strength and modulus, which remain constant even at high temperatures,
- Metal fibers, high strength and resistance to high temperatures,
- Alumina fiber, with excellent resistance to high temperatures,
- Boron fiber, with high modulus and excellent resistance to buckling,
- Polymeric fibers, mainly Aramid, with high strength and modulus.

The mechanical properties of the fibers employed as reinforcement in PMCs are given in Table 2.2.

Table 2.2 Mechanical properties of commercial fibers [6].

Fiber Type	Density (Mg/m3)	Tensile Modulus (GPa)	Tensile Strength (GPa)	Specific Modulus ($m*10^5$)	Specific Strength ($m*10^5$)
GLASS & QUARTZ					
E Glass	2.54	69	2.4	27	0.9
S Glass (Owens Corning)	2.55	86	3.45	34	1.4
Quartz (Quartz& Silica)	2.2	69	3.69	31	1.7
ARAMID					
Kevlar 149	1.47	179	3.45	122	2.3
Twaron HM	1.45	121	3.15	83	2.2
Kevlar 29	1.44	58	3.62	40	2.5
CARBON					
UHM (Thornel P-120S)	2.18	827	2.2	379	1.0
UHM (Celion GY-80)	2.18	572	1.86	291	0.9
UM (Microfil 55)	1.83	379	3.45	207	1.9
IM (Magnamite IM 8)	1.8	303	5.3	168	2.9
SM (Torayca T300)	1.75	230	3.53	131	2.0

Table 2.2 (continued)

Fiber Type	Density (Mg/m3)	Tensile Modulus (GPa)	Tensile Strength (GPa)	Specific Modulus ($m*10^5$)	Specific Strength ($m*10^5$)
LM (Kureha T101 F)	1.65	33	0.79	20	0.5
CERAMIC					
Silicon carbide (Nicalon)	2.55	193	2.76	76	1.1
Alumina-Silicate (Saffil)	3.3	300	2.0	91	0.6
Silicon-Titanium (Tyranno)	2.35	206	2.74	87	1.2
Boron	2.57	400	3.6	156	1.4
METAL					
Stainless Steel Fiber	7.9	197	1.45	25	0.2
Steel, Piano Wire	7.8	207	2.41	26	0.3

2.1.1.3.3. Manufacturing Methods

To fabricate continuous fiber-reinforced PMCs, the very important point is that the fibers should be oriented all in the same direction and should be distributed uniformly throughout the plastic matrix. Various techniques are used for the manufacturing of PMCs. The most common techniques are as follows:

- Hand Lay-Up and Spray-Up
- Sheet Molding Compound
- Bulk Molding Compound
- Autoclave
- Resin Transfer Molding
- Pultrusion
- Filament Winding
- Injection Molding
- Automated Tape Placement

Of these, filament winding is a very important and widely used technique for PMC production and is used for the present investigation.

Filament Winding

Filament winding is a process where the continuous fibers are accurately positioned in a prearranged pattern to form a cylindrical shape. Figure 2.1 shows a basic filament winding process. A number of fiber rovings are pulled from a series of creels and tensioners that control the tension of the fibers into a liquid resin bath that contains the resin itself, the hardeners and the accelerators. At the end of the resin tank, the rovings are pulled through a wiping device where the excess resin is removed from the rovings. Once the rovings are thoroughly impregnated and wiped, they are collected together in a flat band, pass through the carriage and located on the mandrel. The traversing speed of carriage and the winding speed of the mandrel are controlled to generate the desired winding angle patterns. After the appropriate number of layers has been applied, curing is carried out in an oven or at room temperature, after which the mandrel is removed [2].

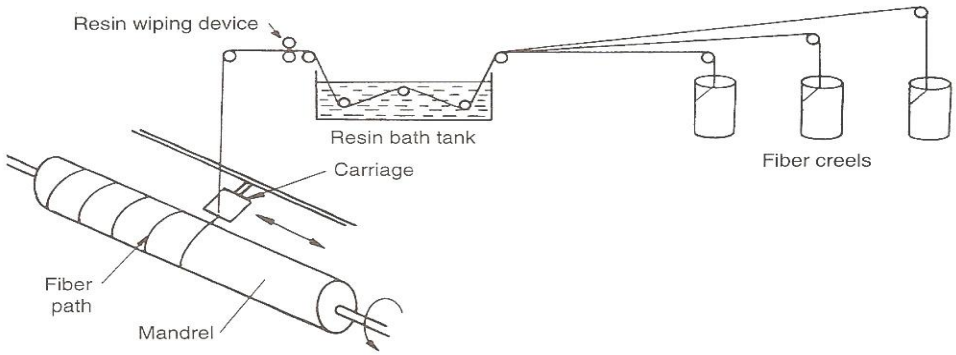

Figure 2.1 Basic filament winding process [7].

The filament winding method in general, has several advantages over other methods. The foremost advantages can be listed as:

- It is highly repetitive and precise in fiber placement.
- It can use continuous fibers to cover the whole component area, which simplifies the fabrication process of many components and increases reliability and lowers the cost by reducing the number of joints.
- It is less labor intensive, which reduces the costs significantly.
- Large and thick walled structures can be built.

The cons of the method may be listed as follows:

- The shape of the component must be chosen in a way that it can be removed from the mandrel.
- Generally, reverse curvatures cannot be wound.

- The mandrel used generally is complex and expensive.
- Surface quality is low.

The filament winding process can be classified as polar and helical winding. In polar winding, delivery head travels around a slowly indexing mandrel, whereas in helical winding, fiber is fed from a horizontally translating delivery head to the rotating mandrel.

Polar Winding: In polar winding, the carriage rotates around the longitudinal axis of a stationary (but indexable) mandrel. After each rotation of the carriage, the mandrel is indexed to advance one fiber bandwidth, so that the fiber bands lie adjacent to each other and there are no crossovers. A complete wrap consists of two plies oriented at plus and minus the wind angle on the two sides of the mandrel. In contrast with helical winding, polar windings are employed with lower wind angles. Figure 2.2 shows polar winding.

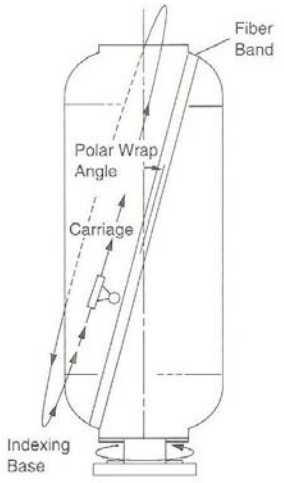

Figure 2.2 Polar winding [7].

Helical Winding: This type of winding requires a system capable of laying down a band in helical patch over the surface of the turning mandrel, turning it around on the end, and returning to the starting position to repeat the cycle. The angle of roving band with respect to the mandrel axis is called the wind angle [7]. By adjusting the speed of the carriage and the rotational speed of the mandrel, any wind angle between 0^o and near 90^o can be obtained. The mechanical properties of the composites that are wound helically strongly depend on the wind angle. Besides being the predominant filament winding method, there are a number of limitations to helical winding, which include the machine bed size, mandrel weight and turning diameter clearances. Figure 2.3 shows helical winding.

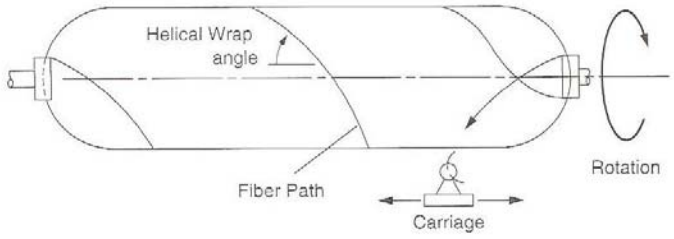

Figure 2.3 Helical winding [7].

Hoop (Circumferential) Winding: In hoop winding, which is a specialized helical winding technique, bands are wound almost perpendicular to the mandrel axis, that is, the winding angle approaches to 90^o. In production, hoop windings are generally associated with other wind angles as they provide a significant reinforcement in hoop direction.

2.2. Mechanical Characterization of Filament Wound Tubes

It is essential to know the mechanical characteristics of filament wound tubes in order to employ them in design applications. Based on this fact, several tests are performed on composite structures.

2.2.1 Test Methods and Their Standards

The one most common testing method is the split ring test. The test is done according to ASTM D2290-04, to determine the apparent hoop tensile strength. The test is mainly for most of the plastic products utilizing a split disk test fixture under defined conditions of pretreatment, temperature, humidity and test machine speed [8].

In order to determine the hydraulic pressure that produces failure of either thermoplastic or reinforced thermosetting resin pipe, tubing, or fittings in a short time period, tests according to ASTM D1599 is employed. This test method is used for determination of the resistance of either thermoplastic or reinforced thermosetting resin pipe, tubing, or fittings under hydraulic pressure for short time periods. The standard gives two procedures; Procedure A is used to determine burst pressure if the mode of failure is to be determined. Procedure B is used to determine the compliance of the component with the minimum burst requirements [9].

Cyclic pressure tests are done according to ASTM D2143-00 Standard, titled as "Test Method for Cyclic Pressure Strength of Reinforced, Thermosetting Plastic Pipe". The standard describes the methods for the determination of the failure characteristics of reinforced plastic pipe when subjected to cyclic internal hydraulic pressure. It is limited to pipe in which the ratio of outside diameter to wall thickness is 10:1 or more [10].

The standard ASTM D2992-01, "Standard Practice for Obtaining Hydrostatic or Pressure Design Basis for Fiberglass (Glass-Fiber-Reinforced Thermosetting-Resin) Pipe and Fittings" is another standardized test method that is employed in the

determination of mechanical properties of polymer matrix composites. The practice given in the standard is for two procedures, namely Procedure A (cyclic) and Procedure B (static) loading. It is used for obtaining a hydrostatic design basis for fiberglass piping products, by evaluating strength-regression data derived from testing pipe or fittings, or both, of same materials and construction, either separately or in assemblies. The standard is also applicable for both glass-fiber-reinforced thermosetting-resin pipe and glass-fiber-reinforced polymer mortar pipe [11].

In order to determine the tensile properties of the filament wound composite tubes, ASTM standard D2105-01 (Standard Test Method for Longitudinal Tensile Properties of Fiberglass (Glass-Fiber-Reinforced Thermosetting-Resin) Pipe and Tube) is used. The method discussed in the standard covers the determination of the comparative longitudinal tensile properties of fiberglass pipe when tested under defined conditions of pretreatment, temperature, and testing machine speed. Both glass-fiber-reinforced thermosetting-resin pipe (RTRP) and glass-fiber-reinforced polymer mortar pipe (RPMP) are classified as fiberglass pipes [12].

Another important property, creep life for the filament wound tubes can be determined experimentally according to the ASTM standard F948-94(2001)e1, titled "Standard Test Method for Time-to-Failure of Plastic Piping Systems and Components Under Constant Internal Pressure With Flow". This test method discusses the determination of the time-to-failure of plastic piping products under constant internal pressure and flow [13].

The compressive properties of the polymer matrix composites are determined according to the ASTM standard D3410/D3410M-03; "Standard Test Method for Compressive Properties of Polymer Matrix Composite Materials with Unsupported Gage Section by Shear Loading". The standard describes the in-plane compressive properties of polymer matrix composite materials reinforced by high-modulus fibers. The composite material forms are limited to continuous-fiber or discontinuous-fiber reinforced composites for which the elastic properties are specially orthotropic with

respect to the test direction. The test procedure introduces the compressive force into the specimen through shear at wedge grip interfaces. This type of force transfer differs from the procedure in Test Method ASTM D695 where compressive force is transmitted into the specimen by end loading [14].

A very important property, fatigue properties of the polymer matrix composites can be evaluated employing the ASTM standard D3479/D3479M-96(2002)e1, titled "Standard Test Method for Tension-Tension Fatigue of Polymer Matrix Composite Materials", within the scope of determination of the fatigue behavior of polymer matrix composite materials subjected to tensile cyclic loading. The composite material forms are limited to continuous-fiber or discontinuous-fiber reinforced composites for which the elastic properties are especially orthotropic with respect to the test direction. The test method discusses the unnotched test specimens subjected to constant amplitude uniaxial in-plane loading where the loading is defined in terms of a test control parameter [15].

For determination of the shear properties of the polymer matrix composites, tests according to the ASTM D3518/D3518M-94(2001) standard can be employed. The standard is titled as "Standard Test Method for In-Plane Shear Response of Polymer Matrix Composite Materials by Tensile Test of a $\pm 45^{o}$ Laminate", and the test is developed for the determination of the in-plane shear response of polymer matrix composite materials reinforced by high-modulus fibers. The composite is limited to a continuous-fiber reinforcement of +45° laminate, capable of being tension tested in the laminate direction [16].

2.2.2 Literature Survey on Mechanical Characterization of Filament Wound Tubes

Considering the importance of knowing the mechanical characteristics of filament wound tubes in applications, there is a considerable amount of work carried out in literature on this subject. In most of the studies, mechanical constants and

characteristics are determined by means of several mechanical tests and analytical studies. P. Mertiny, F. Ellyin, and A. Hothan studied the effect of multi axial filament winding on tubular structures of three different winding configurations by comparing the data of [±45, $\pm 60_2$] and [±30, $\pm 60_2$] with [$\pm 60_3$], so called baseline data, under constant ratios of biaxial loads [17]. In this work, two types of failures are distinguished; functional failure, where leakage of test fluid takes place but the structure still carries load, and structural failure, where the specimen can no longer carry any load. The writers evaluated the experimental hoop and axial stresses at both functional and structural failure, derived the elastic constants for pure hoop and axial loading conditions and studied the failure envelopes. It was concluded that the failure modes depend strongly on applied stress ratio, and matrix damage can be minimized using [±30, $\pm 60_2$] configuration. [±45, $\pm 60_2$] and [±30, $\pm 60_2$] configurations showed higher functional and structural strength compared to the baseline configuration under hoop-to-axial load ratios smaller than 1, due to the reduced axial strain in ±60 covers; whereas the baseline configuration performed best under pure hoop loading condition. Multi angle winding configurations exhibit improved strength especially in [2H:1A] loading condition, which is often the case in tubular pressure vessels.

Another study performed to obtain experimental data that represents the effect of winding angle on the mechanical properties of filament wound composites that are subjected to uniaxial and biaxial stresses is carried out by P. D. Soden et. al [18]. Biaxial loading (hoop and axial loadings) for lined and unlined specimens at different winding angles and uniaxial compression is applied to tubular specimens. Electrical resistance strain gages are attached to some of the specimens during testing and the data obtained are evaluated to determine elastic constants. Accordingly, stress-strain curves are plotted using the strain data from the strain gages and the axial stress and hoop stress data evaluated from the burst tests. The data obtained are compared with the results of relevant studies and conclusions are made considering all the literature and experimental data. The work also discusses the variation of the failure stresses at different tests, effect of the wall thickness on the compressive

properties, effect of stress concentrations through the gauge length and compares the stress envelopes in the work and literature for different winding angles. It was concluded that the test specimens without internal liners could withstand lower loads due to the leaking at the matrix cracks. The leakage and fracture strengths are affected considerably with winding angles while winding angle has a slight effect on axial compression strength. Larger winding angles increases the tube's uniaxial tensile strength in the hoop direction whereas decreases uniaxial tensile strength in axial direction. Also, the stress-strain analysis showed that elastic constants vary with winding angle as expected from laminate theory. Another study performed by the writers discussed the experimental failure stresses for ±55° filament wound glass fiber reinforced plastic tubes under biaxial loads [19]. For that, axial loads are applied, accompanied with the internal pressure, and the applied circumferential stress to axial stress ratio is kept constant throughout the tests. ±55° filament wound tubes are tested under different stress ratios and the failure test results are recorded. The work described the first stage and final failure modes of the ±55° specimens and the theoretical stress distributions; and discussed the effects of stress distribution on strength, the scatters in failure stresses, and compared them with the previous results. It is stated that when applied hoop stresses are low, the strength of the tube is reduced considerably. The uniaxial compressive strength is almost twice the uniaxial tensile strength but the axial compressive strength is reduced by the presence of high circumferential stresses, unlike the axial tensile strength. For uniaxial tension and compression, there was no evident difference between the initial and final failure stresses. Also, it is shown that the maximum hoop strength occurred between the circumferential to axial stress ratios of 3:1 and 3.5:1 whereas the maximum axial strength occurred at a circumferential to axial stress ratio of 2:1.

F. Ellyin, M. Carroll, D. Kujawski and A.S. Chiu studied the behavior of multidirectional filament wound glass fiber/epoxy tubular structures under biaxial loading [20]. The study aims to investigate the effects of the rate and ratio of biaxial loading on failure strength, damage accumulation and monotonic stress - strain behavior of glass fiber reinforced epoxy tubes. To do that, different hoop to axial

stress ratios are employed in testing; failures are studied and biaxial failure envelopes of stress and strain are developed and interpreted. It was concluded that strength and stiffness are functions of biaxial stresses, failure modes and damage accumulations at failure are dependent on biaxial stress ratio, and linear elastic behavior of the tubes can only be observed at relatively low temperatures.

In the study of N. Tarakçioğlu, L. Gemi and A. Yapıcı, the fatigue behavior of glass fiber reinforced ±55° filament wound composite tubes is investigated experimentally [21]. The specimens produced from E-glass fiber with epoxy resin are tested at an open ended internal pressure apparatus and the fatigue tests are performed according to the ASTM standard D2992. In the study, six different stress levels based on different percentages of the static strength of the specimen were applied at one frequency. During testing, three damage mechanisms are observed. These mechanisms are identified as crazing, leakage and final failure; and the number of cycles to these predetermined levels are investigated and recorded. In addition, S-N curves are drawn for each damage stage. In the study, it was shown that there is an analogy between macro and micro damage stages of the specimens. In addition, at higher stress levels, the final failure of the specimen occur just after the leakage whereas for low stress levels, there is much more cycles in between leakage and final failure stages.

A. S. Kaddour, M. J. Hintonand P. D. Soden studied experimentally the behaviour of ±45° glass/epoxy filament wound composite tubes under quasi-static equal biaxial tension–compression loading [22]. Test are performed on ±45° tubes under 1:−1 stress ratio, unidirectional lamina (circumferentially-wound tubes) under torsion, ±45° angle ply filament wound tubes under uniaxial tension and ±45° angle ply filament wound under stress ratio SR=2.3:−1. The writers gave the necessary equations describing the unidirectional shear stress and strain values obtained from tests on tubes under various loadings conditions first, and then considering the experimental results, they obtained the pressure, load and stress-strain curves and examined failure appearances. Considering this data, comparison is made between

the shear stress–strain curves extracted from tests and the work discussed the factors affecting the behaviour of specimens under biaxial loadings: buckling of specimens, effects of bulging, effects of scissoring, effects of thermal stresses, effects of transverse stress component and effects of micro cracking.

Biaxial fatigue behavior of a multidirectional filament-wound glass fiber/epoxy pipe is studied by F. Ellyin and M. Martens [23]. In their study, the writers aimed to investigate the fatigue life and leakage behavior of a multidirectional filament wound, glass fiber reinforced epoxy tube by determining the deformation behavior of the pipe under different applied biaxial stress ratios, leakage curves and leakage envelopes for each applied stress ratio, and micro and macro failure modes by physical observation and measured parameters. The test specimen configuration was $[\pm 66_4, 0, \pm 66_3, 0, \pm 66_3, 0, \pm 66_5]$. It was shown from the biaxial fatigue tests that the decrease in secant modulus with cyclic loading and the leakage are strongly dependent on both the applied maximum biaxial stress and the applied biaxial stress ratio. Also, in all cases of loading, there was a significant decrease in the secant modulus which stabilizes after a certain period and this reduction indicates that indicate that there is a relation between the stress ratio and the maximum applied stress and the largest initial reduction was observed in the axial secant modulus under pure axial loading and in the hoop secant modulus under pressure vessel type loading (2.5H:1A). Another consequence of the results is that the damage, which ranged from a uniform matrix cracking to a delamination with pinhole bursting or a combination of both, is dependent on the maximum applied stress. The observed damage indicated that the amount of axial tension in the specimen governs the uniformity of the matrix cracking, where internal pressure governed the amount of delamination.

Another study, carried out by C. Kaynak and O. Mat, discussed the effect of stress level and loading frequency on the fatigue behavior of filament wound composite tubes [24]. In their work, tensile tests were applied to the tubular test specimens and the number of cycles to three predetermined fatigue damage stages (crazing in the matrix, crazing along the fiber winding direction leading to debonding, and fiber

breakage and total failure) were monitored as a function of test frequency and stress level. In the study, it was shown that fatigue resistance of the composite tubes decreased considerably when the stress level was increased and life increases as the loading frequency was raised.

J. Bai, P. Seeleuthner, and P. Bompard studied in detail the mechanical behavior of ±55° filament wound glass fiber/epoxy resin tubes [25]. The tube was made of six plies of ±55° winding angle. A series of mechanical tests were performed under different loading conditions; pure tensile loading, pure internal pressure and combined loading. The work discussed the damage mechanisms under these conditions. It is stated that the damage and failure process can be described by three steps: initiation of the damage process by microcracking, delamination between the different plies, and development and coalescence of cracks and delaminations in different plies. Also, it is confirmed that at that zones free of fibers, matrix cracks occur perpendicular to the tensile direction, at the zones where fiber volume fraction is low, microcracks propagated around fiber bundles, and at the zones of high fiber volume fraction, the microcracks propagated at the fiber/matrix interfaces.

M.R. Etemad, E. Pask and C.B. Besant described an experimental and computational work to determine the hoop strength and other mechanical properties like tensile modulus, tensile strength and Poisson's ratio of two carbon fiber reinforced composite in their work [26]. Experimental results showed that hoop winding should be reinforced with axial winding, where computational work showed that these reinforcements should be principally in the bore section.

In literature, the mechanical characteristic of filament wound pressure vessels are not only studied by experimental work, but analytical procedures, numerical solutions and finite element analysis are commonly employed in characterization. L. Parnas and N. Katırcı analyzed the cylindrical pressure vessels by thin wall and thick wall solutions [27]. They developed an analytical procedure for the design and prediction of behavior of fiber-reinforced composite pressure vessels under combined

mechanical and hygrothermal loading. The writers employed the classical lamination theory and generalized plane strain model in the formulation of the elasticity problem. A cylindrical shell having a number of sub-layers, which are cylindrically orthotropic, is regarded as in the state of plane strain. Loads applied are internal pressure, body force due to rotation, axial force with temperature and moisture variation. In the study, it was concluded that the optimum winding angle for filament wound composite tubes that are subjected to internal loading is 52.1° and 54.2°, which is consistent with the data present in literature. In addition, it was stated that the burst pressure value depends on the analysis method used and thin-wall analysis is said to be an average, but a safe choice.

P.M. Wild and G.W. Vickers studied the analysis of filament wound cylindrical shells under combined centrifugal, pressure and axial loading [28]. The writers developed an analytical procedure to asses the stresses and deformations of filament wound structures under different loading types. The procedure developed is mainly based on classical laminated plate theory, and models both plane stress and plain strain states of a cylindrical shell having a number of sub-layers, which are cylindrically orthotropic. It is concluded that when there is no axial loading, benefit of wind angle variation is more significant. If axial loads are present, the benefits of wind angle variation are more considerable under the last ply criterion.

J.-S Park, C.-S. Hong, C.-G. Kim and C.-U. Kim studied the analysis of filament wound composite structures considering the change of winding angles through the thickness direction [29]. The test specimens are filament wound composite cylinders, but closed at the ends by means of domes. The behavior of the filament wound structure subject to internal pressure was analyzed considering the winding angle change through the thickness. The writers employed finite element analyses considering the change of winding angles through the thickness under internal pressure loads, by a commercial finite element analysis code, ABAQUS and coded a user subroutine to impose the change of winding angles to each solid element. They also performed internal pressure tests and worked to verify the finite element

analysis results considering geometrical nonlinearities with the experimental data, and it was shown that the experimental results showed good agreement with the analysis results. It was concluded that it is required to consider the winding angle change through the thickness direction for the precise prediction of stress distribution over the domes and near the openings in order to not to have the undesirable failures.

C. Gargiulo, M. Marchetti, and A. Rizzo studied on the prediction of failure envelopes of composite tubes, which are subjected to biaxial loadings [30]. The writers worked to provide numerical and experimental data on the strength of carbon fiber reinforced epoxy filament wound tubes. The effects of winding angle on the failure loads are investigated. For that, variety of combinations of internal, external and axial loads are applied on the tests specimens to produce biaxial stress states and test results are examined. Finite element method is also employed and the results of experiments are compared with finite element results. Different damage and failure mechanisms for different winding angles and loading conditions are discussed and failure envelopes are obtained.

Another study that is performed by M. Xia, K. Kemmochi and H. Takayanagi, discusses the analysis of filament-wound fiber-reinforced sandwich pipes [31]. The work analyzes the stresses and strains of a filament-wound sandwich pipe subjected to internal pressure and thermo-mechanical loading, based on the classical laminated plate theory in detail, and give the numerical results and discussions. It is concluded that netting analysis can be employed for the design of the optimum winding angle, which depends upon geometry and construction materials and also, for a thick-walled laminate-ply sandwich pipe, a 55° winding angle is no longer an ideal arrangement. In addition, it was stated that, under internal pressure loads, the axial strain of the pipe studied changes from positive to negative with respect to the winding angle.

X.-K. Sun, S.-Y. Du, and G.-D Wang discussed the bursting problem of filament wound composite pressure vessels by using nonlinear finite element method [32]. By this method, the writers calculated the stresses and the bursting pressure of filament

wound composite pressure vessels. During failure analysis, maximum stress failure criteria and stiffness-degradation model are employed. It was concluded that the design method from the equivalent case to its real one is not sensible. To obtain the optimum structure, all affecting factors should be considered in detail.

The above summary shows that there is source of information on the performance of internally pressurized composite tubes. Most applications require the estimation of life cycle performance of these composite tubes. This work is the first step to generate data for a future work that would be used in health monitoring investigations and life studies based on these methods.

CHAPTER III

EXPERIMENTAL WORK

This chapter will cover the experimental work carried out; the test specimens and testing procedure in detail. Test specimen design, manufacturing and nomenclature, strain measurements, testing procedure and reporting will be discussed.

3.1 Test Tube (Specimen) Design

Internal pressure tests are extensively employed in mechanical characterization of composite tubes. The method generates stresses in the material, primarily in the hoop direction, and provides important information on the mechanical properties of the tubes that are subjected internal pressure.

As discussed in several scientific works and commercial standards, to obtain reliable data, the test should be carried out within some predefined constraints, which will be discussed in the next paragraphs. These constraints are taken into consideration for the test specimen design, and the design is optimized by improving some details.

One important point that should be considered is that, during internal pressure testing, stress concentration arises around the end closure grips. This phenomenon may lead the specimen failing at the stress concentrated region in a non-homogeneous way, which surely affects the test results and reliability of the data, in view of not obtaining the expected fracture type. For the design of an effective internal pressure test specimen, it should be guaranteed that uniform stresses are obtained through the test section and that failure takes place within the gauge length. To assure this, specimen end reinforcements that reduce the stress concentration effect around the end closures are employed in the tests. A straight reinforcement

would cause a similar stress concentration effect at the points where it ends, and accordingly the reinforcements are designed in a stepped manner, where the wall thickness gradually decreases with distance through the specimen length, at both ends and at some point, homogenizes with the gauge length, that is, the specimen wall thickness.

Another point is that the failures in the tests are expected to be catastrophic, that is, bursting is desired, and any condition that shall not permit that, should be prevented. However, leakage at the matrix cracks during internal pressure loading, and not being able to obtain catastrophic failure is a serious problem that is encountered in internal pressure tests of composite materials. To avoid the possible leakage of test fluid; thus an unwanted failure mode, an elastomeric liner is placed in the specimen. During loading, the internal liner is filled with the test fluid and pressurized. The liner, whose load carrying capacity is neglected in the work, also helps preventing the leakage of test fluid through the end gripping units during loading.

Another modification that is done is the reinforcement of all specimens with a single layer of hoop winding as the outermost layer. This revision is considered when it was observed that other winding angles result in quite irregular and rough surfaces, which affects the test results. Application of a single layer of 90° reinforcement winding would not only give rise to a much smoother outer surface, but also decreases the possibility of fluid leakage in the cases where an internal liner is absent in internal pressure loadings. Hoop layers contribute to the strength of the total tube. Indeed; such hoop reinforcement layers are present nearly in all pressure vessel applications as the outermost layer.

The test specimens are hollow, open-ended cylindrical tubes. They are of 400 mm total length, and have an internal diameter of 60 mm, which is the outer diameter of the mandrel employed in filament winding operation. The gauge length, which is the length between the reinforcements employed, is 200 mm. The wall thicknesses

depend on the process parameters like tensioning condition and winding angle, and the type of reinforcement. The geometry of the test specimen is given in Figure 3.1.

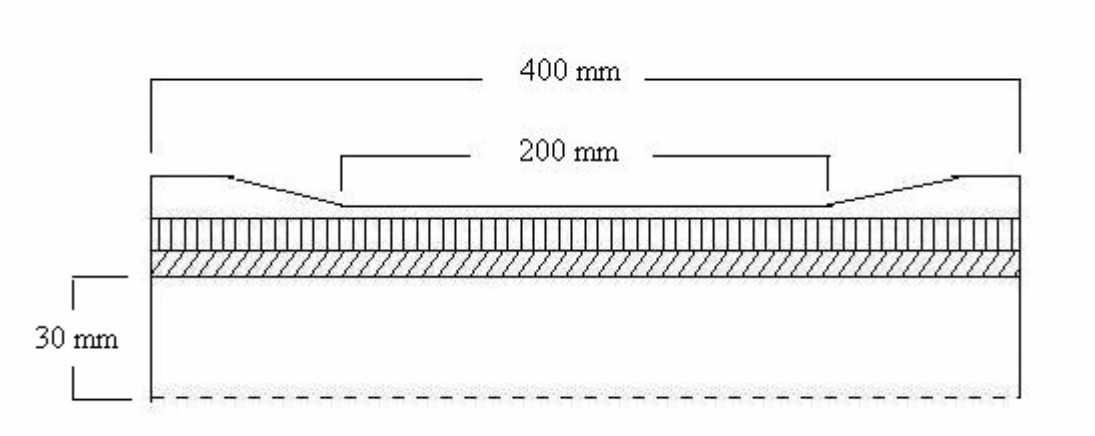

Figure 3.1 Internal pressure test tube.

3.2 Test Setup

Internal pressure tests are performed according to ASTM D 1599-99 standard. The setup is composed of pressurizing system, test fixtures, strain gauge data acquisition components and pressure recording units.

3.2.1 Pressure Test Setup

The internal pressure is applied by a micro-processor controlled 2000 Bar hydraulic testing machine at the test facilities of BARIŞ Electrical Industries. The system records the change in internal pressure with time during the test, until the specimen fails, and so the bursting pressure. The system is accredited by METU Mechanical Engineering Department. The pressure test system is given in Figure 3.2 and the schematic view of the system is given in Figure 3.3.

Figure 3.2 Internal pressure test system.

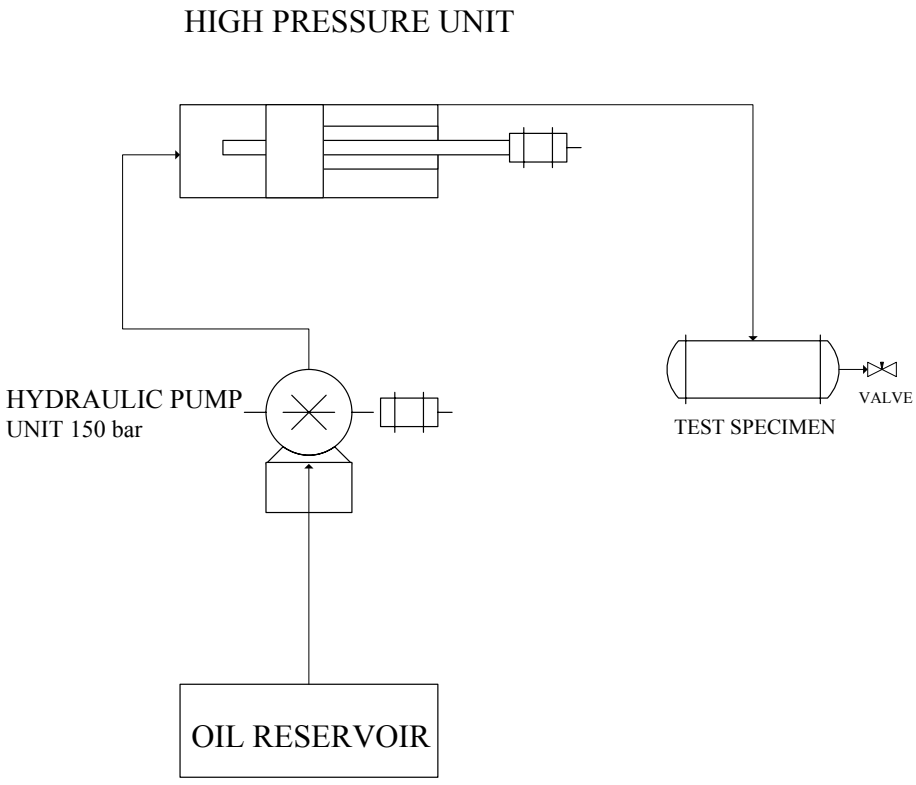

Figure 3.3 Schematic view of the pressure test system.

3.2.2 Test Fixtures

For the application of internal pressure efficiently, the specimen should be fixed properly to the test apparatus. The fixing should be strong enough to avoid leakage of test fluid, fracture or slip of the specimen at the matching region.

ASTM D 1599-99 standard offers two types of end conditions for internal pressure testing: fixed end condition where the expansion in axial direction is hindered by fixing the ends to each other, and open end condition, where there is no constraint on the test specimen in axial direction.

The first system design was a fixed end gripping system that fixes the test specimen at both ends, and thus restricts the motion in longitudinal direction. This was attained by matching the two end units by means of metal bars. The system effectively gripped the test specimens, but during loading, it was noticed that the specimen expands considerably at the middle part in hoop direction and touches the metal bars that are used for fixing the end closures to each other. This resulted in a significant stress concentration at those points and a consequent early failure of the specimens. Later the design has been changed, where one end of the test specimen is fixed to the test unit, while it goes free on the other. This allowed the specimen expansion in the longitudinal direction freely and eliminated the former significant swelling and consequent early failure problem. Another point that is considered in employing this design is that in open end condition, the hoop to axial stress ratio is 2:1, which is the case in pressure vessels, and thus it simulates the pressure vessel better. Accordingly, the tubes are fixed to the test system by means of the latter gripping end closure unit for this test, which is presented in Figure 3.4.

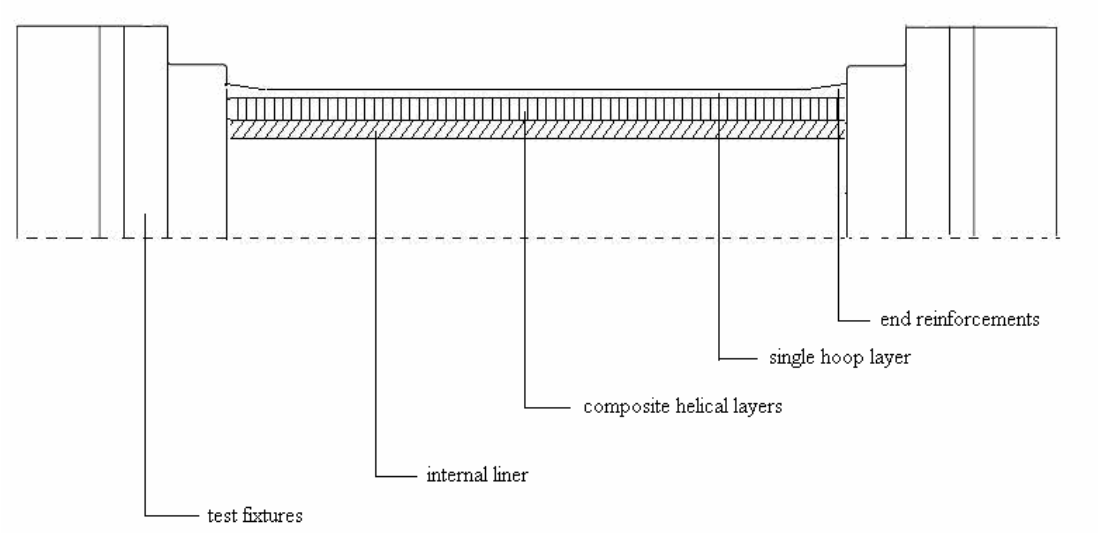

Figure 3.4 Tube with the test fixtures.

3.2.3 Strain Gauge Data Acquisition System

The strain gauge data acquisition software is an 8 channel add-on card product of PC-LabCards. The software uses Equation (3.1) for measurements.

$$\frac{\Delta R}{R} = k\varepsilon_0 \tag{3.1}$$

where

ΔR = resistance variation,
R = gauge resistance,
k = gauge factor,
ε_o = strain.

The software lets the user to adjust the record speed and the bridge voltage value. Gauge resistance R and gauge factor k are identified and set by the user, and ΔR, the variation in resistance is measured. In the hardware, there lies a dummy strain gauge, and the system measures the difference of the resistances of the dummy strain gauge and the actual strain gauge, ΔR. The software then evaluates the data and gives the strain, ε_o as the output.

3.3 Specimen Manufacturing

The tubes that are employed in internal pressure tests are manufactured by utilizing the filament winding technique, in the production facilities of BARIŞ Electrical Industries.

3.3.1 Filament Winding Machine

The tubes are manufactured at a three axial computer controlled Bolenz & Schafer wet filament winding machine. Maximum winding diameter of the machine is 500 mm and the maximum winding length is 4500 mm. The system is capable of utilizing winding angles from 0° to 90° and its carriage receives the fibers from four creels. The winding speed of the system is maximum 60m/min and it can carry a mandrel of maximum 1000 kg. during the winding process, the system controls the fiber tension and the temperature of the resin bath, up to 100°C. The filament winding machine is given in Figure 3.5.

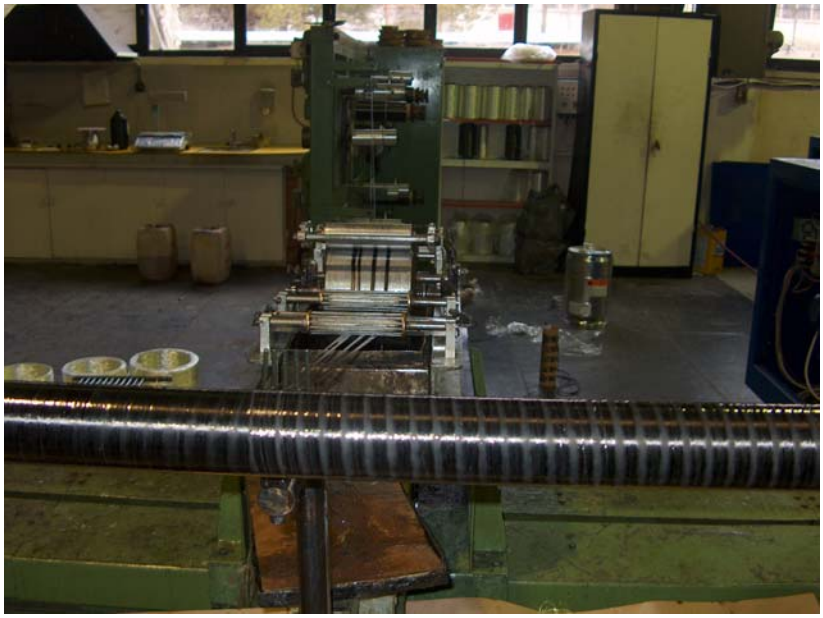

Figure 3.5 Three axial computer controlled Bolenz&Scafer filament winding machine.

3.3.2 Tooling

Filament winding operation is performed on a 60 mm diameter steel mandrel. The total length of the mandrel is 243 mm, and the winding length is 196 mm. The net length, which gives the length of the tubes manufactured, is 160 mm. Figure 3.6 gives the schematic view of the mandrel.

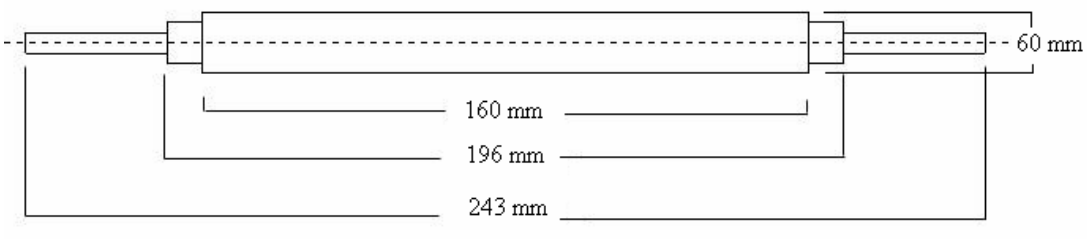

Figure 3.6 Schematic view of the steel mandrel.

3.3.3 Filament Winding

Test tubes are manufactured by using an epoxy resin system with two different fiber types, where, for each type, five different helical winding angles are used. As a process parameter, extra tensioning is applied to fibers for some of the tubes during manufacturing in order to observe the effect of wetting. The properties of the resin system and the reinforcements employed in are as follows:

Resin System

The resin system employed in the fabrication of the tubes is CIBA Araldite MY740 (100 parts by weight) – Hardener HY918 (85 parts by weight) – Accelerator DY062 (0.2 – 2.5 parts by weight) mixture; a hot curing, low-viscosity impregnating resin system. The system is characterized by its good mechanical and dielectric properties and good aging resistance and is suitable for filament winding, wet laminating, and pultrusion processes. The properties of the system are given in Table 3.1.

Table 3.1 Mechanical properties of the resin system employed.

Property	**Unit**	**MY740 – HY918 – DY062 RESIN SYSTEM**
Glass Transition Temperature	(C)	123
Max. Tensile Stress	(MPa)	61
Elongation At Break	(%)	2
Elastic Modulus	(MPa)	3637

Reinforcements

The reinforcements employed in the fabrication of the tubes are PPG Roving 1084 2400 TEX glass fiber; continuous product of PPG Industries, and Grafil 800 TEX carbon fiber, continuous product of TOHO-TENAX. The properties of the reinforcements are given in Table 3.2.

Table 3.2 Mechanical properties of the reinforcements employed.

Property	**Unit**	**GRAFIL 800 TEX CARBON FIBER**	**PPG 2400 TEX GLASS FIBER**
Max. Tensile Stress	(MPa)	4900	2600
Elongation At Break	(%)	2	4 – 5
Elastic Modulus	(MPa)	240000	73000

During the manufacturing of the test tubes, five different winding angles are employed; 25°, 45°, 54°, 65°, 90°. To increase the strength of the tubes in hoop direction and have a smooth surface, one hoop layer is wound on each of them, as discussed in the previous sections.

Tensioning is applied to the fibers while they are pulled from the creels, in order to get a better wetting of fibers by the resin. In the study, tensioning is used as a parameter to observe the effect of wetting on mechanical properties. Accordingly, for both fiber types, five different winding angles and two fiber tensioning levels, tubes are tested. Extra tensioning is applied in a way that, weights of 1.5 kg each are hung on four creels that supply the continuous fibers to the resin bath and then the winding unit during fabrication. The tension values measured are given in Table 3.3.

Table 3.3 Measured tension values for the fibers.

Fiber Type	Number of Fiber Bands	Measurement Location	Extra Weight (kg)	Tension Value
carbon	1	creel	1.5 kg	1100 cN
carbon	2	creel	1.5 kg (x2)	2350 cN
carbon	1	creel	-	800 cN
carbon	2	creel	-	1550 cN
carbon	1	creel	-	1600 cN
glass	4	resin bath	-	49.3 kg
glass	4	resin bath	1.5 kg (x4)	-
glass	2	resin bath	1.5 kg (x2)	45.2 kg
glass	2	resin bath	1.5 kg (x2)	-
glass	2	resin bath	-	5100-5200 cN
glass	1	resin bath	-	2700 cN
glass	1	resin bath	1.5 kg	3500 cN

After the winding operation, the tubes are placed in the furnaces which are given in Figure 3.7 for curing. Curing operation is carried out at 80°C for two hours, and then at 120°C for another two hours. Once the curing is completed, the mandrel is removed from the tubes and the composite hollow tubes are handled.

Figure 3.7 Curing furnaces.

To sum up, considering these production parameters, twenty tubes are fabricated by employing two different reinforcement types, two different tensioning conditions and five different winding angles.

3.3.4 Cutting the Tubes and Grinding of End Reinforcements

Once the tubes are manufactured and cured, they are then cut into the desired length by means of mechanical cutting, each tube to give three test tubes. To have good fit in the test fixtures, the reinforcement regions are grinded.

Test tubes are given in Figure 3.8.

Figure 3.8 Test tubes.

3.4 Tube Nomenclature

Considering the manufacturing parameters, a designation system is developed for the tests. This system identifies the test tubes by the fiber type, winding angle, the tensioning condition, and the position in the full length tube. The fiber type is designated by the letter “E” followed by the numbers 1 or 2, which are assigned to carbon fiber and glass fiber, respectively. The latter letter “G” specifies the tension setting; 1 stands for no external tensioning and 2 stands for tensioned condition. Winding angle is next, called by the letter “A” and followed by 1, 2, 3, 4 or 5, which are the winding angles of 25^{o}, 45^{o}, 54^{o}, 65^{o}, 90^{o} respectively, remembering all the tubes of these winding angles are reinforced with a single layer of hoop winding as the outermost layer. The one last number after the dash shows the position of the test tube obtained by sectioning the manufactured tubes into three parts. For example, the tube that is reinforced with glass fiber, manufactured with extra tensioning, wound at an angle configuration of [±54°/90], and was at the middle position of the manufactured tube obtained from filament winding machine, is designated as E2G2A3-2.

3.5 Strain Measurements

In the present work, UFRA-5-350-23 rosette type electrical resistance strain gauges are employed for recording the strain data. The main test materials for the strain gauge are metals, ceramics and composites. Operating temperature range of the gauge is -20 to +150°C and the strain limit is 3% (30000×10^{-6}). Strains in axial and hoop directions can be measured simultaneously by the mentioned system. Figure 3.9 shows the UFRA-5-350-23 strain gauges.

Figure 3.9 Schematic representation of UFRA-5-350-23 strain gauge

For the installation of strain gauges, grease, rust, etc. at the bonding surface are removed. The bonding surface is lightly polished with an abrasive paper to obtain a smoother surface. Having a perfectly smooth surface is vital in strain gauge installations because the quality of the bonding of the strain gauge to the test surface is directly related with the smoothness of the surface. The strain gauges are fixed on the tubes by their special CN adhesive. The lead wires originated from the strain gauges are soldered to the connecting terminals of the strain gauge data acquisition system. The acquisition system collects and records the data coming from each three measurement units.

3.6 Testing Procedure

The internal pressure tests are performed according to the standard ASTM D1599-99, “Standard Test Method for Resistance to Short-Time Hydraulic Pressure of

Plastic Pipe, Tubing, and Fittings". The method covers the determination of the resistance of either thermoplastic or reinforced thermosetting resin pipe, tubing, or fittings to hydraulic pressure in a short time period, and consists of loading the tube to failure in a short time interval by means of a hydraulic pressure.

The internal pressure test experimentation was carried out in the following sequence:

- The tubes that are fabricated by wet filament winding method and cut into desired length are fixed to the end closures by means of an adhesive. The adhesive employed is CIBA – GEIGY Araldite AV 138–Hardener HV 998 epoxy adhesive. Once the adhesive is applied, the tube and the end closure system are placed in the furnace at 80°C for one hour to allow the adhesive to cure.
- The internal liner is placed in the tube.
- The strain gauge is fixed in the middle portion of the tube by using its CN adhesive.
- It is filled completely with water.
- The tube is attached to the hydraulic pressure system assuring no air is entrapped.
- The cables originated from the connecting terminals of the data acquisition system are connected to the strain gauges by soldering.
- Pressure is applied and increased uniformly and continuously, until the tube fails. Meanwhile, the pressure increase and changes in the strain are monitored and recorded.
- Using the necessary formulations, the strain and pressure data are evaluated to obtain the mechanical characteristics.

3.7 Testing Reporting

For the internal pressure test, the pressure is increased uniformly and continuously by means of the hydraulic test unit. Meanwhile, the strain data is recorded as well.

When the test ends, the pressure drops to zero and recording of strain data is ended. Tests are reported as mentioned in ASTM D 1599-99 standard. By the end of the test, the pressure and strain gauge data are studied in order to obtain the desired mechanical parameters.

3.7.1 Record of the Data

The tube dimensions are noted before the internal pressure test starts. Once the test starts, the internal pressure system and the strain gauge system start to record the pressure and strain data simultaneously, and they continue recording until the tube fails and the loading rate is recorded as well. After the failure, the maximum pressure recorded and the failure modes are also reported.

The internal pressure system records a single pressure value each second, until the tube fails. These pressure values are recorded in bars. The computer program returns the pressure data in the form of a text document. The pressure recording system is given in Figure 3.10.

Figure 3.10 Pressure recording system.

The strain gauge data acquisition system records three data for each three measurement units per second and it returns the strain data in the form of a text document. For the evaluation of data, in order to have a consistency with the pressure values, the corresponding data recorded per second is considered for all measurement units. The strain gauge data acquisition system is given in Figure 3.11.

Figure 3.11 Strain gauge data acquisition system.

3.7.2 Calculations

Pressure test system records the pressure data in bars. The hoop stresses that are formed in the tubes are calculated according to the ASTM D1599-99 standard [9], by using Equation (3.2).

$$S = \frac{P(d+t)}{2t} \tag{3.2}$$

where

S = hoop stress, MPa
P = internal pressure, MPa
d = average inside diameter, mm
t = minimum wall thickness, mm

More commonly, Equation (3.3) is employed in the hoop stress calculations. But in order to keep consistency with the ASTM 1599-99 standard, Equation (3.2) is used in this work.

$$S = \frac{Pd}{2t} \tag{3.3}$$

where

S = hoop stress, MPa
P = internal pressure, MPa
d = average inside diameter, mm
t = minimum wall thickness, mm

After converting the pressure values that are recorded in bars into stress values, stress-strain curves are plotted for each test by employing the converted stress data and the strain data that are recorded from the strain gauges. Hoop elastic constants of the curves are evaluated and these results will be given in the following chapter.

CHAPTER IV

EXPERIMENTAL RESULTS

This chapter presents the internal pressure test results and the hoop elastic constants determined experimentally for the test tubes. The bursting pressure test results then will be represented in terms of performance factor, to form a reliable basis for discussion of data in the next chapters.

4.1. Internal Pressure Test Results

In this section, the internal pressure test results for all the test tubes are presented, in two major groups regarding their reinforcement types. The burst pressure data with the data of maximum strain, which is formed during loading, are given.

4.1.1 Carbon Fiber Reinforced Tubes

Twenty three internal pressure tests are applied on Carbon fiber reinforced epoxy tubes. The test results data for the tubes are given in Table 4.1. For the tubes where strain gauge is damaged and stopped collecting data, “maximum strain formed” column is left empty. The tests are recorded to be successful if bursting is achieved. For the tubes E1 G2 A2 – 2, E1 G1 A3 – 1, E1 G1 A3 – 2, and E1 G2 A3 – 2, bursting could not be achieved, but instead, the adhesive that is used to fix the test tube to the end closure units could not be able to withstand the load and failed, resulting in a sudden decrease in internal pressure. The tests performed on these tubes are recorded to be unsuccessful, as the desired failure mode is not obtained.

In all tests, the pressure values that are recorded in bars are converted into stress values, and compared them with the data obtained from strain gauges. The stress – strain data for the carbon reinforced tubes of $[\pm 25°]_3$ $[90°]_1$, $[\pm 45°]_3$ $[90°]_1$, $[\pm 54°]_3$ $[90°]_1$, $[\pm 65°]_4$ $[90°]_1$ and $[90°]_7$ winding angle configurations is given in Figures 4.1, 4.2, 4.3, 4.4 and 4.5, respectively.

Table 4.1 The test results for carbon fiber reinforced tubes

Test Tube Number	Maximum Strain Formed (mm/mm)	Maximum Strain Recorded (mm/mm)	Average Outer Diameter (mm)	Average Loading Rate (bars/sec)	Loading Time (sec)	Maximum Pressure Recorded (bars)	Test Result
E1 G1 A1 - 1	0.012000	0.012000	64.66	10.5	14	147	SUCCESSFUL
E1 G1 A1 - 2	0.010200	0.010200	64.63	6.3	18	114	SUCCESSFUL
E1 G1 A1 - 4	0.010300	0.010300	63.26	9.1	13	118	SUCCESSFUL
E1 G2 A1 - 1	0.010300	0.010300	63.72	6	16	96	SUCCESSFUL
E1 G2 A1 - 2	0.010900	0.010900	63.78	9.8	8	78	SUCCESSFUL
E1 G2 A1 - 3	0.011400	0.011400	63.37	7.6	21	159	SUCCESSFUL
E1 G1 A2 - 1	-	0.012400	63.39	12.3	34	418	SUCCESSFUL
E1 G1 A2 - 2	0.012900	0.012900	63.74	13.6	31	422	SUCCESSFUL
E1 G2 A2 - 1	-	0.012900	63.56	14.2	29	382	SUCCESSFUL
E1 G2 A2 - 2	-	0.012700	63.51	13.9	29	**404-NO FAILURE**	UNSUCCESSFUL
E1 G1 A3 - 1	0.006980	0.006980	63.2	12.5	30	**372-NO FAILURE**	UNSUCCESSFUL
E1 G1 A3 - 2	0.008300	0.008300	63.22	13.1	30	**392-NO FAILURE**	UNSUCCESSFUL
E1 G1 A3 - 3	0.007910	0.007910	63.26	13.1	43	540	SUCCESSFUL
E1 G2 A3 - 1	0.000327	0.000327	63.25	13.1	38	498	SUCCESSFUL
E1 G2 A3 - 2	0.007910	0.007910	63.14	13.5	29	**390-NO FAILURE**	UNSUCCESSFUL
E1 G1 A4 - 1	0.000669	0.000669	63.63	11.8	12	141	SUCCESSFUL
E1 G1 A4 - 2	0.000766	0.000766	63.63	10	14	140	SUCCESSFUL
E1 G2 A4 - 1	0.001230	0.001230	63.73	8.9	15	134	SUCCESSFUL
E1 G2 A4 - 2	0.000822	0.000822	63.83	8.1	17	137	SUCCESSFUL
E1 G1 A5 - 1	0.001260	0.001260	63.9	1.7	10	17	SUCCESSFUL
E1 G1 A5 - 2	0.000707	0.000707	63.78	2	11	22	SUCCESSFUL
E1 G2 A5 - 1	0.001290	0.001290	62.72	3.7	7	26	SUCCESSFUL
E1 G2 A5 - 2	0.000216	0.000216	62.94	2	11	22	SUCCESSFUL

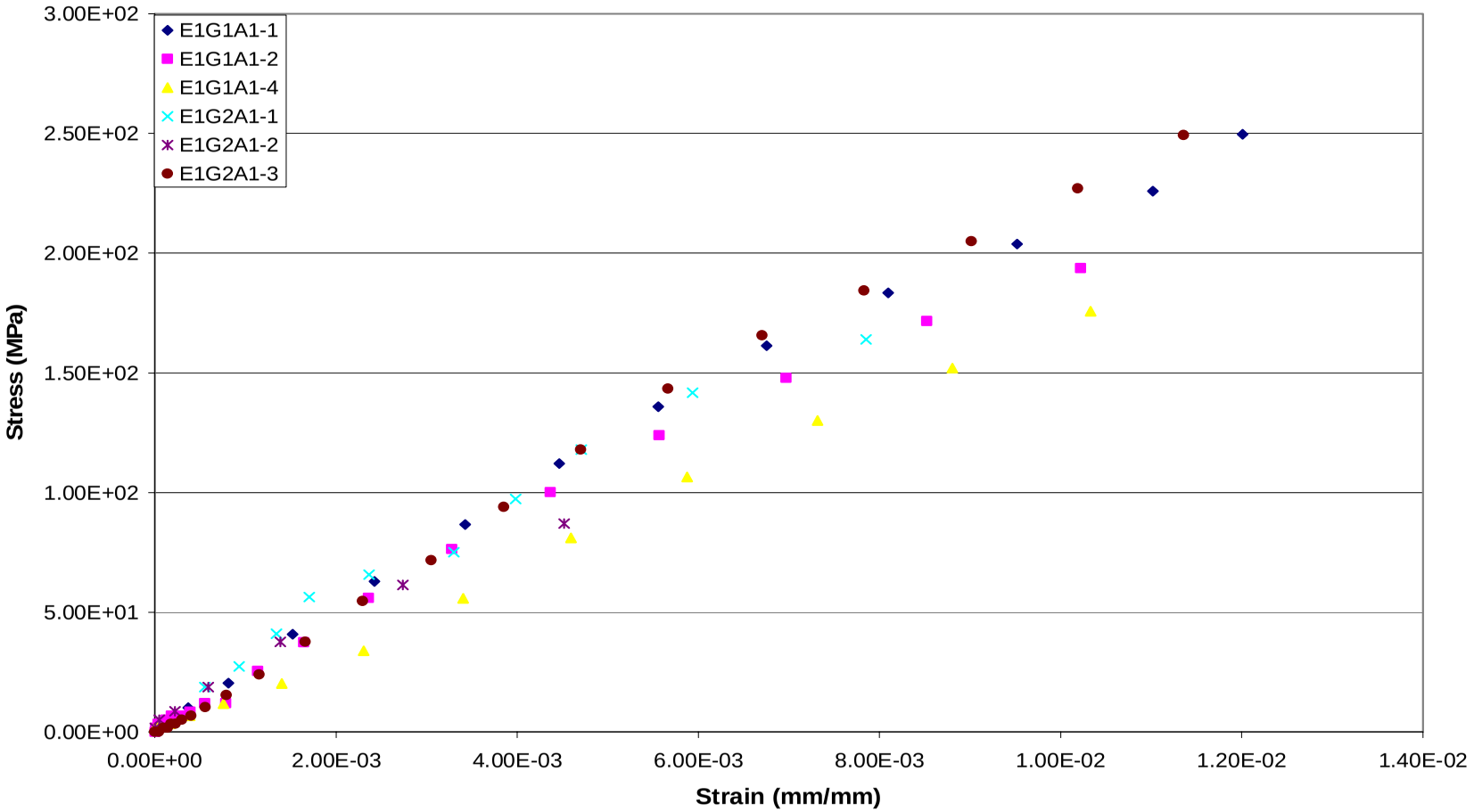

Figure 4.1 The stress – strain data for the carbon reinforced tubes of $[\pm 25°]_3\,[90°]_1$ winding angle configuration

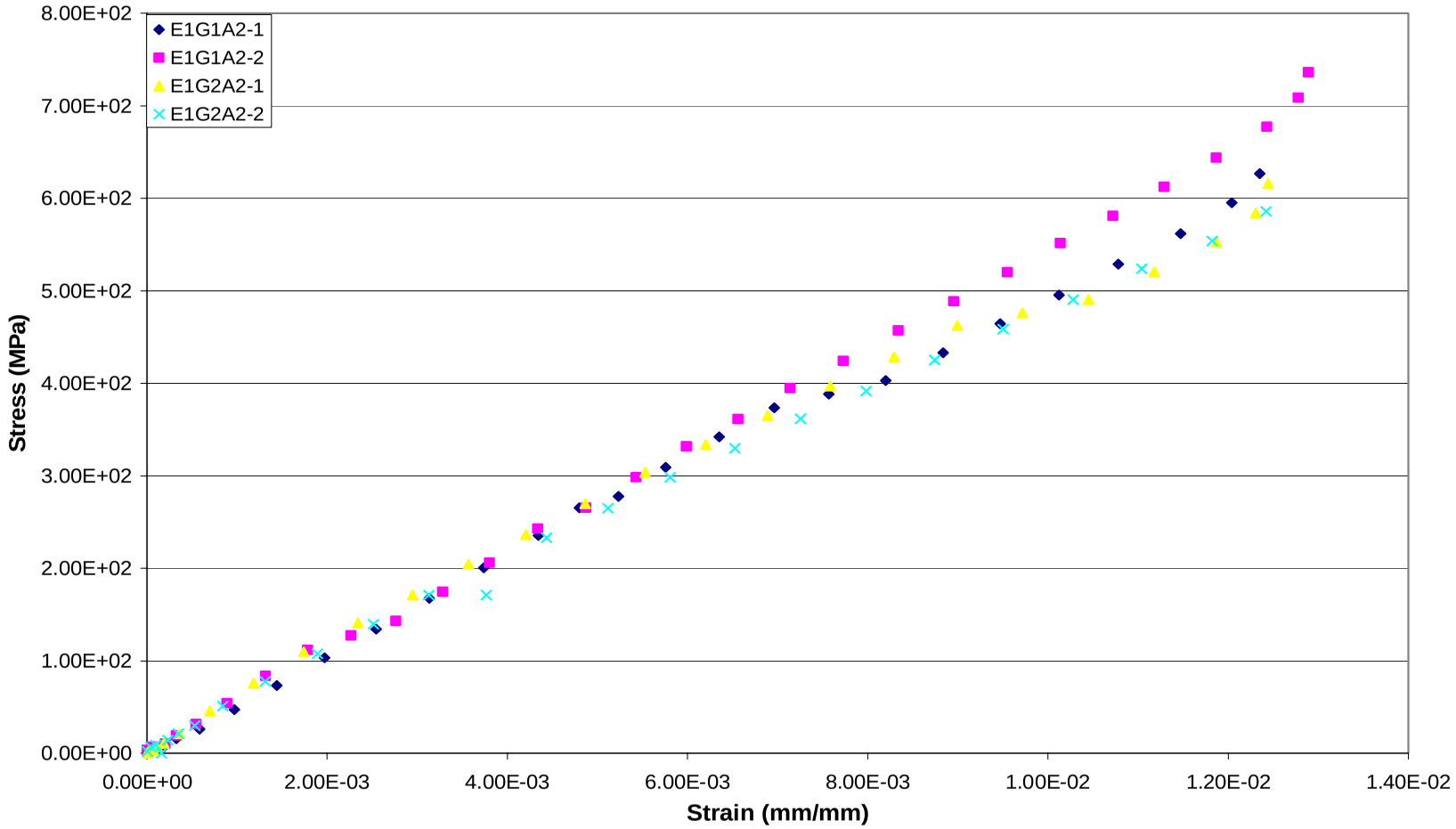

Figure 4.2 The stress – strain data for the carbon reinforced tubes of $[\pm 45°]_3\,[90°]_1$ winding angle configuration

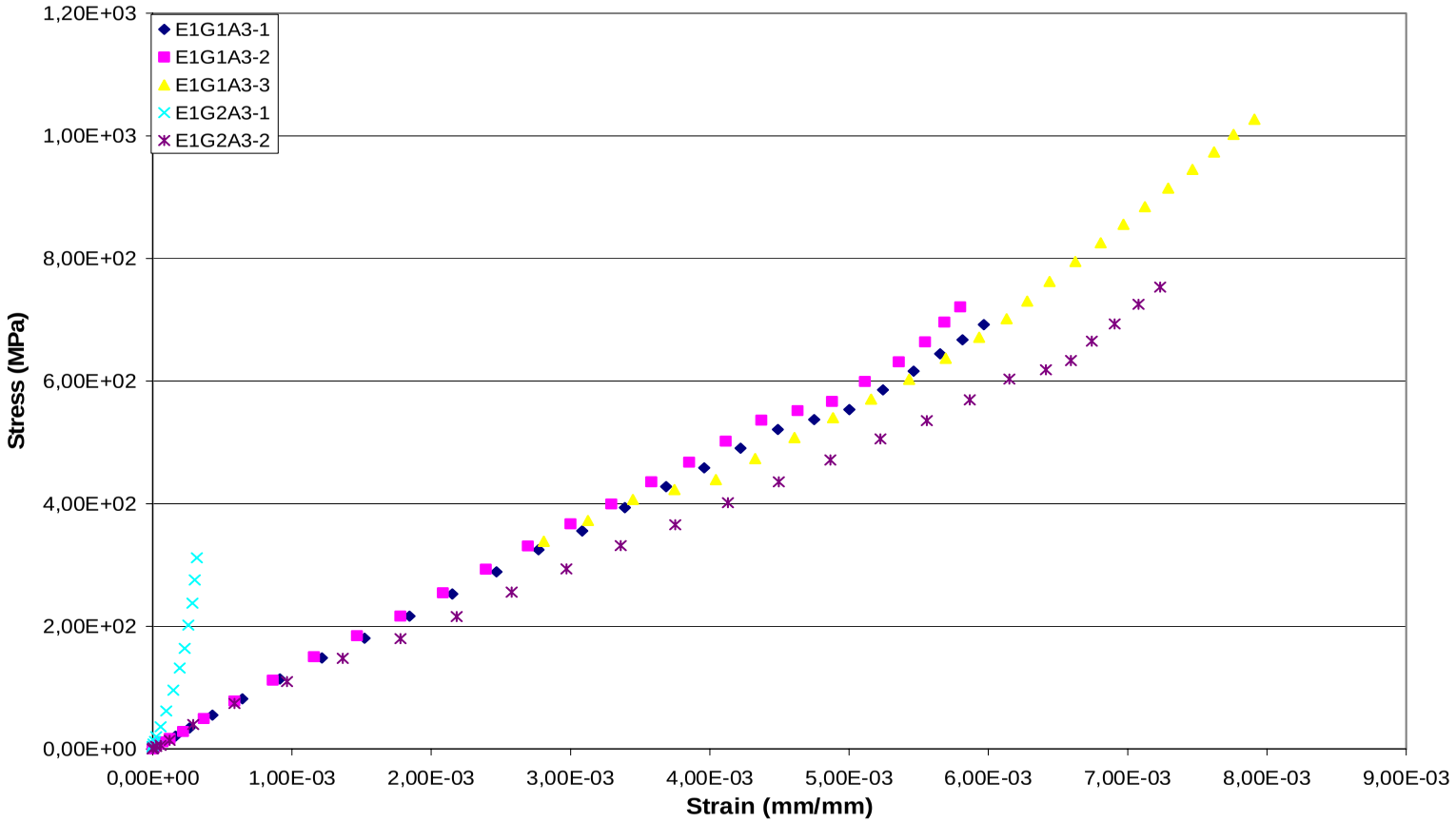

Figure 4.3 The stress – strain data for the carbon reinforced tubes of $[\pm 54°]_3\,[90°]_1$ winding angle configuration.

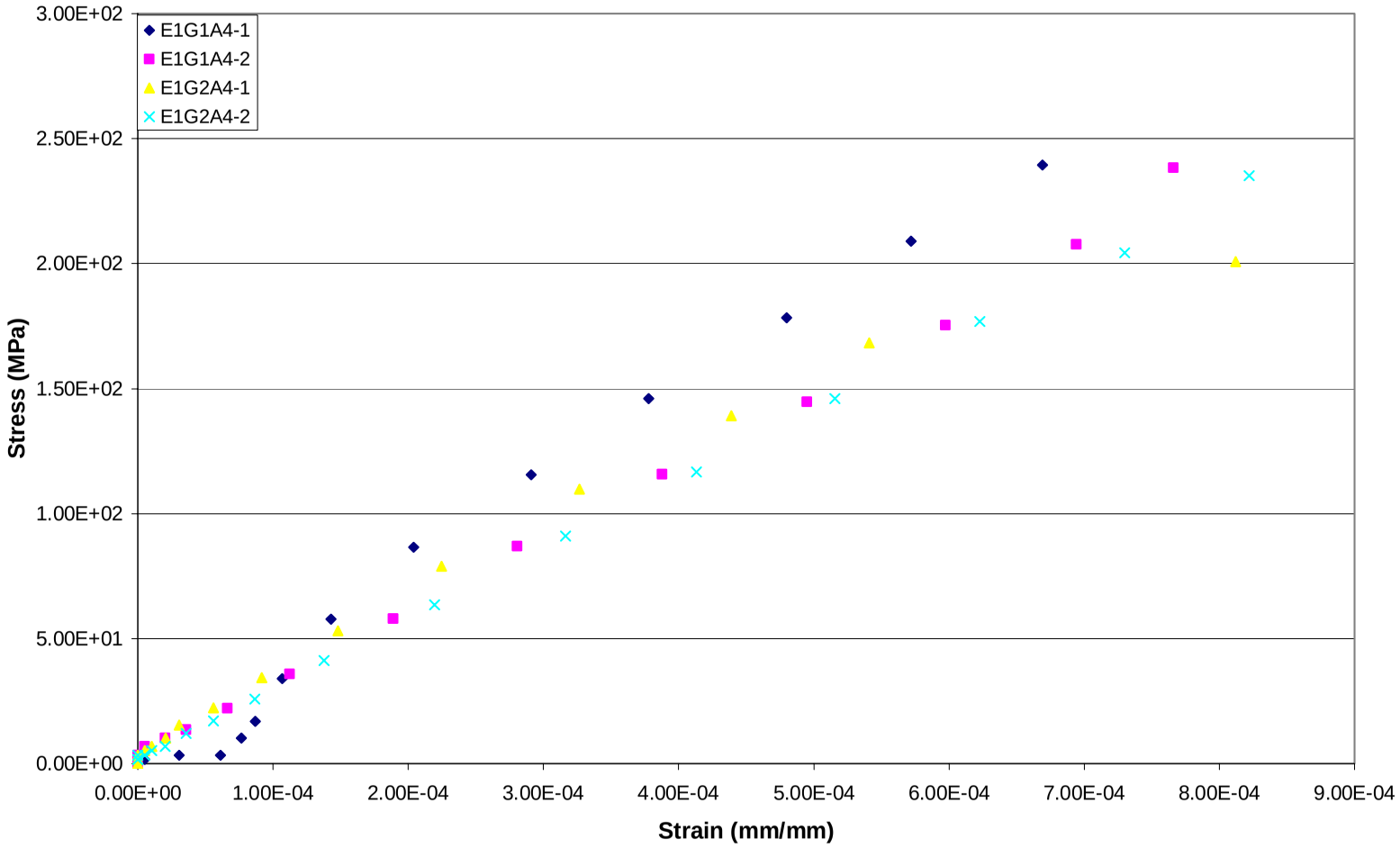

Figure 4.4 The stress – strain data for the carbon reinforced tubes of $[\pm 65°]_4\,[90°]_1$ winding angle configuration.

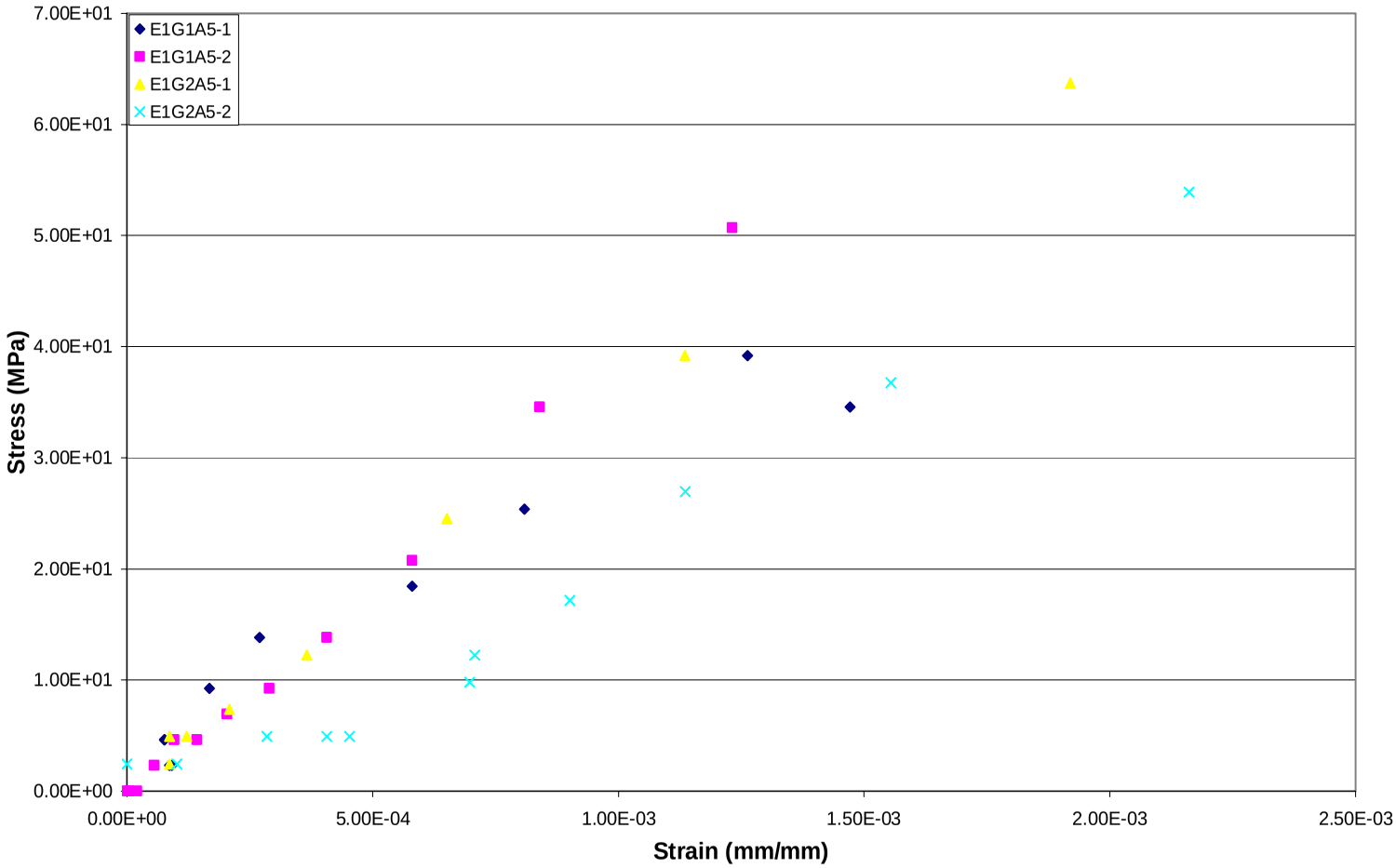

Figure 4.5 The stress – strain data for the carbon reinforced tubes of $[90°]_7$ winding angle configuration.

4.1.2 Glass Fiber Reinforced Tubes

Thirty internal pressure tests are applied on glass fiber reinforced epoxy tubes. The test results data for the tubes are given in Table 4.2. For the tubes E2 G2 A2 – 1, E2 G2 A2 – 5, E2 G1 A3 – 1, E2 G1 A3 – 2 and E2 G1 A3 – 4, bursting could not be achieved, but instead, the adhesive that is used to fix the test tube to the end closure units could not be able to withstand the load and failed, resulting in a sudden decrease in internal pressure. The tests performed on these tubes are recorded to be unsuccessful, as the desired failure mode is not obtained. The pressure values for the tubes E2 G2 A1 – 2, E2 G2 A1 – 4 and E2 G2 A2 – 2 could not be recorded due to a problem in the internal pressure data recording system.

In all tests, the pressure values that are recorded in bars are converted into stress values, and compared them with the data obtained from strain gauges. The stress – strain data for the glass reinforced tubes of $[\pm 25°]_2$ $[90°]_1$, $[\pm 45°]_2$ $[90°]_1$, $[\pm 54°]_2$ $[90°]_1$, $[\pm 65°]_3$ $[90°]_1$ and $[90°]_5$ winding angle configurations is given in Figures 4.6, 4.7, 4.8, 4.9 and 4.10, respectively.

Table 4.2 Test results for glass fiber reinforced tubes

Test Tube Number	Maximum Strain Formed (mm/mm)	Maximum Strain Recorded (mm/mm)	Average Outer Diameter (mm)	Average Loading Rate (bars/sec)	Loading Time (sec)	Maximum Pressure Recorded (bars)	Test Result
E2 G1 A1 - 5	-	0.022400	63.78	8.7	27	236	SUCCESSFUL
E2 G1 A1 - 6	-	0.012600	64.62	7.3	30	220	SUCCESSFUL
E2 G2 A1 - 1	-	0.010500	64.34	6.1	15	91	SUCCESSFUL
E2 G2 A1 - 2	-	0.011900	64.11	-	-	NO PRESSURE DATA	SUCCESSFUL
E2 G2 A1 - 4	-	0.012800	64.85	-	-	NO PRESSURE DATA	SUCCESSFUL
E2 G2 A1 - 5	-	0.012700	64.9	6.7	29	194	SUCCESSFUL
E2 G2 A1 - 6	-	0.010400	64.39	8.7	21	183	SUCCESSFUL
E2 G1 A2 - 1	-	0.012600	64.3	9.3	40	371	SUCCESSFUL
E2 G1 A2 - 2	-	0.012500	64.27	9.9	40	396	SUCCESSFUL
E2 G2 A2 - 1	-	0.012200	63.23	6.9	52	359-NO FAILURE	UNSUCCESSFUL
E2 G2 A2 - 2	-	0.012700	63.34	-	-	NO PRESSURE DATA	SUCCESSFUL
E2 G2 A2 - 3	-	0.011700	64.29	10.5	26	274	SUCCESSFUL
E2 G2 A2 - 4	-	0.012400	64.28	8.9	32	285	SUCCESSFUL
E2 G2 A2 - 5	-	0.012200	64.29	7	23	160-NO FAILURE	UNSUCCESSFUL
E2 G1 A3 - 1	0.006180	0.006180	64.14	8.9	35	410-NO FAILURE	UNSUCCESSFUL
E2 G1 A3 - 2	0.011800	0.011800	63.91	8.5	47	397-NO FAILURE	UNSUCCESSFUL
E2 G1 A3 - 4	-	0.012000	64.28	10	45	450-NO FAILURE	UNSUCCESSFUL
E2 G1 A3 - 5	-	0.012100	64.57	10	43	425	SUCCESSFUL
E2 G2 A3 - 1	-	0.011900	64.14	10.9	24	471	SUCCESSFUL
E2 G2 A3 - 2	0.010900	0.010900	63.94	9.5	43	457	SUCCESSFUL
E2 G1 A4 - 4	0.011400	0.011400	65.17	5.4	21	114	SUCCESSFUL

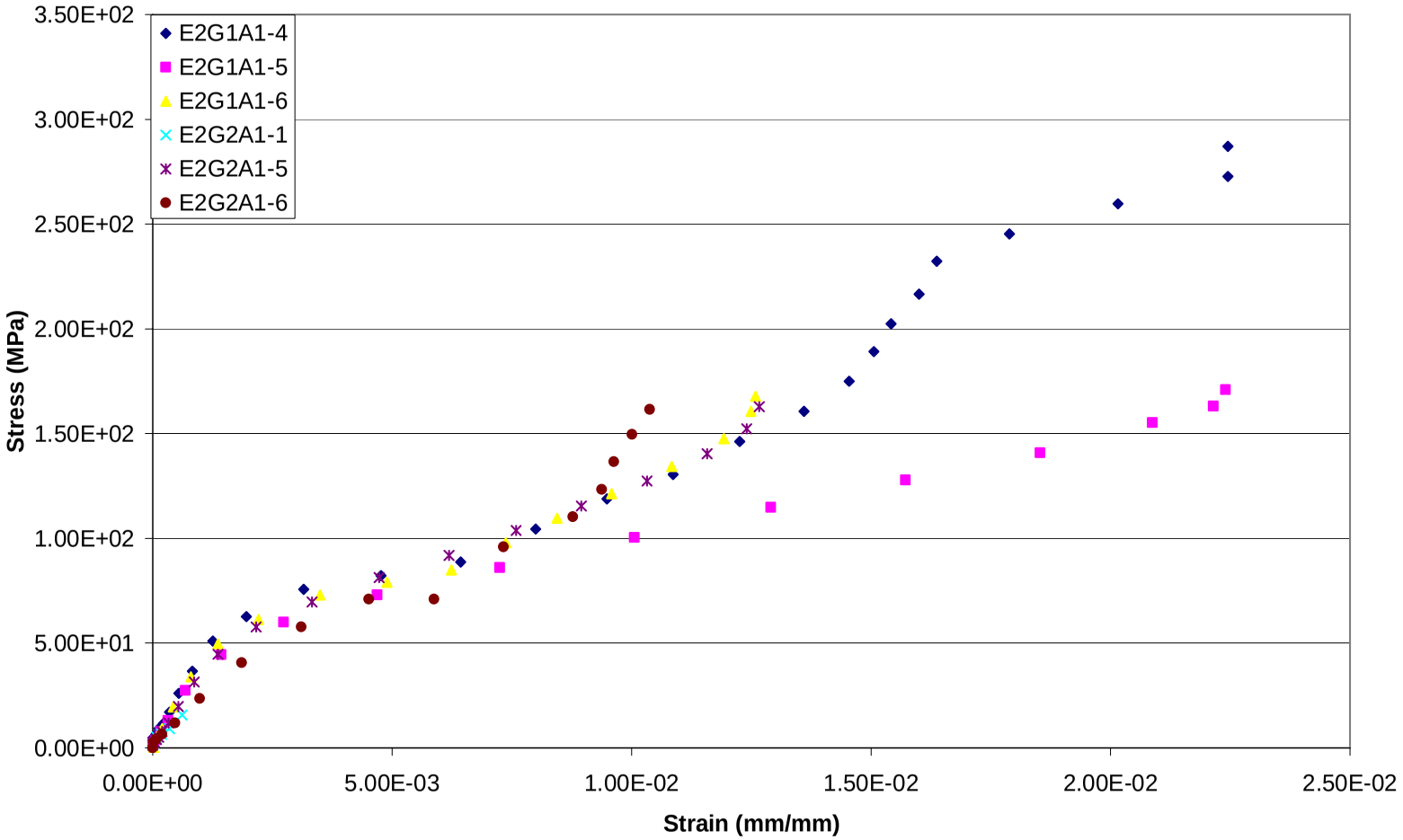

Figure 4.6 The stress – strain data for the glass reinforced tubes of $[\pm 25°]_2\,[90°]_1$ winding angle configuration.

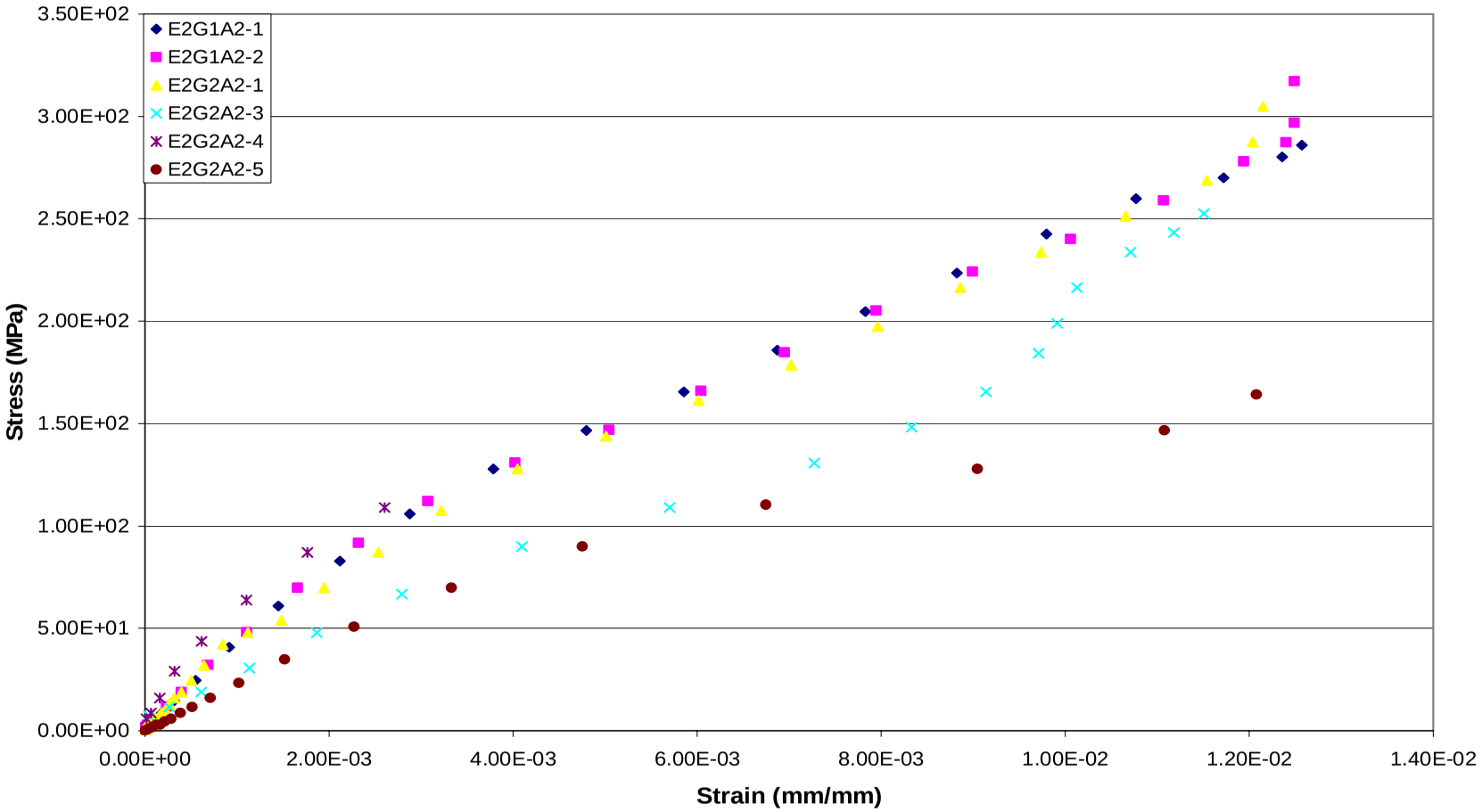

Figure 4.7 The stress – strain data for the glass reinforced tubes of $[\pm 45°]_2\,[90°]_1$ winding angle configuration.

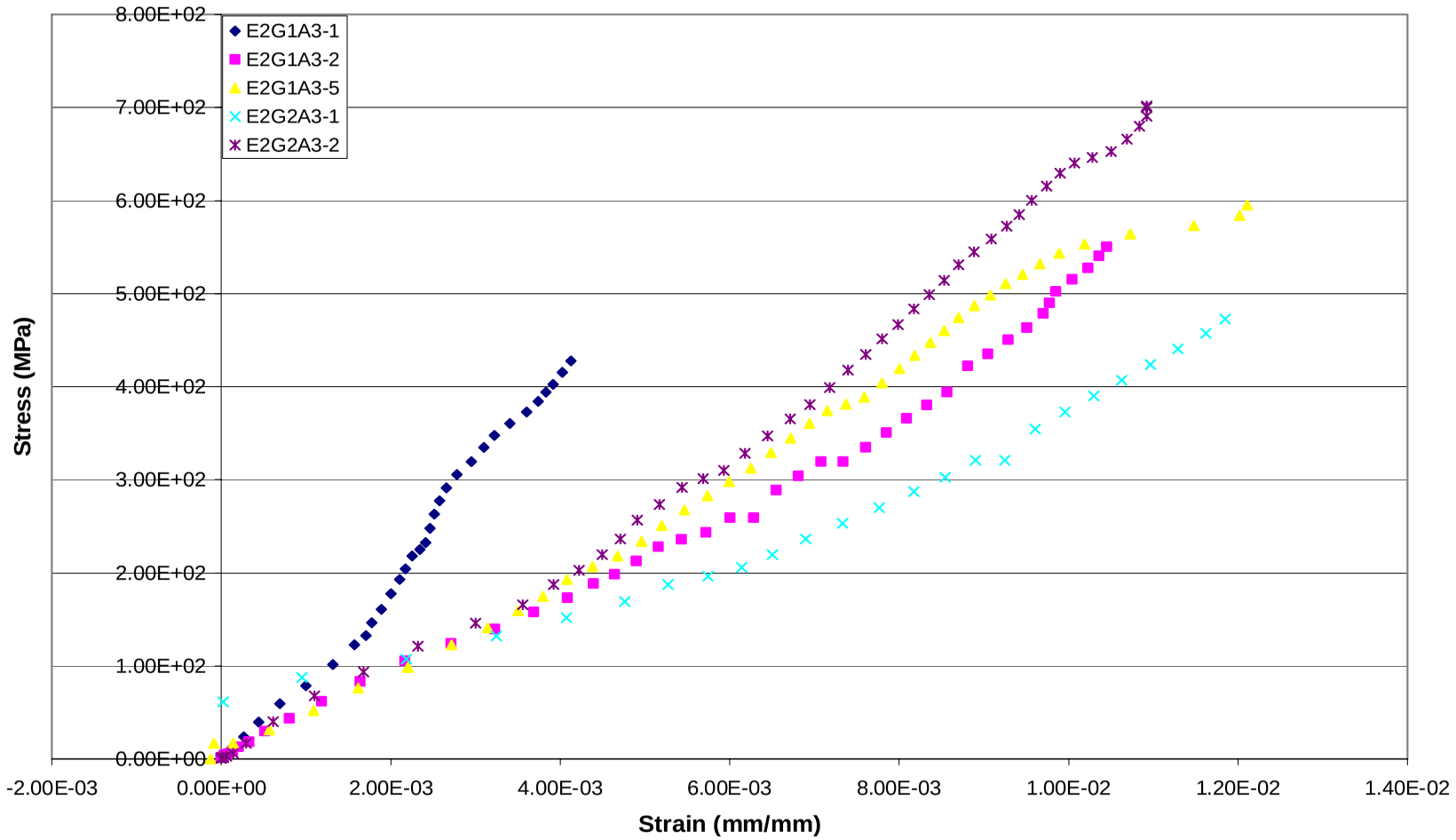

Figure 4.8 The stress – strain data for the glass reinforced tubes of $[\pm 54°]_2\,[90°]_1$ winding angle configuration.

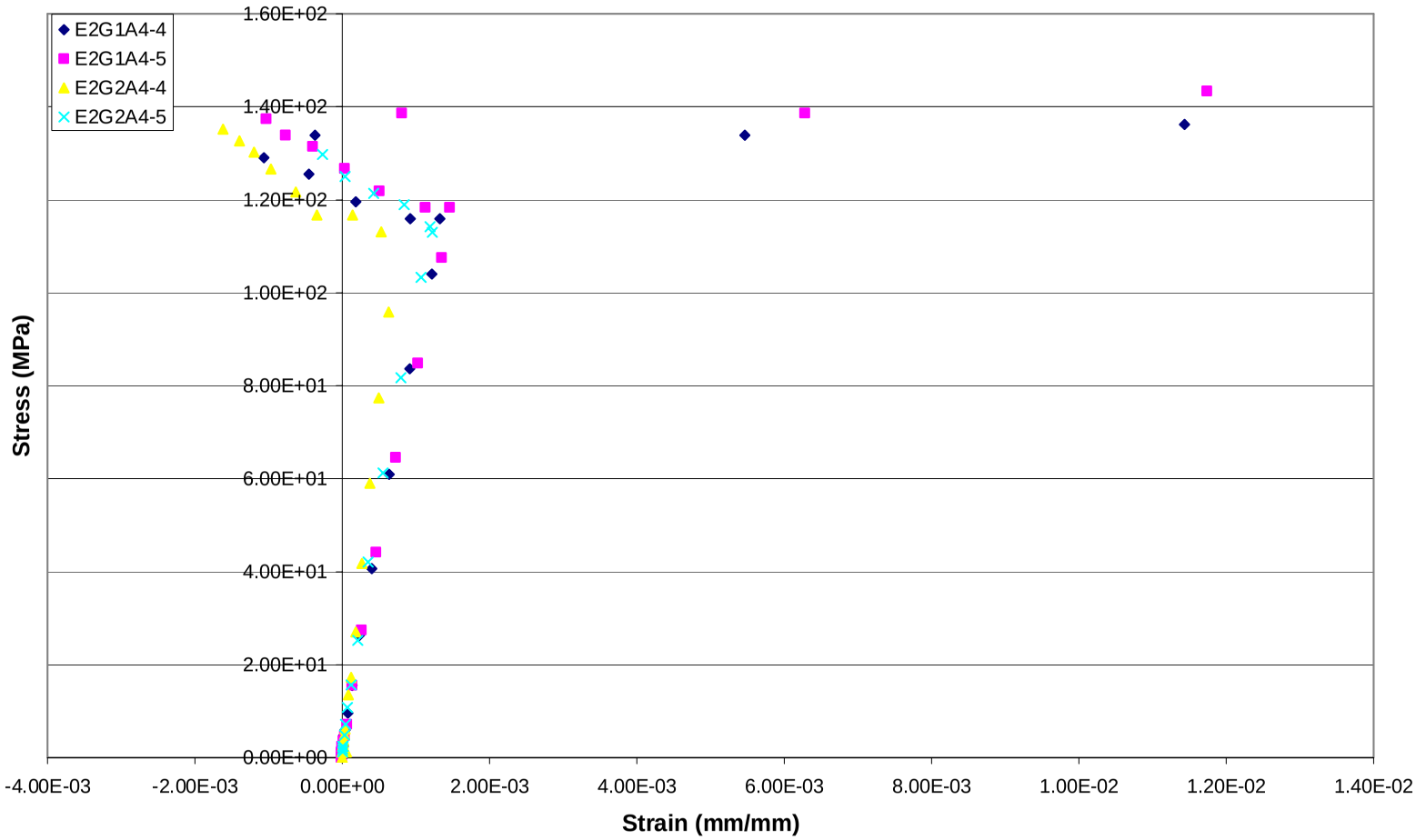

Figure 4.9 The stress – strain data for the glass reinforced tubes of $[\pm 65°]_3\,[90°]_1$ winding angle configuration.

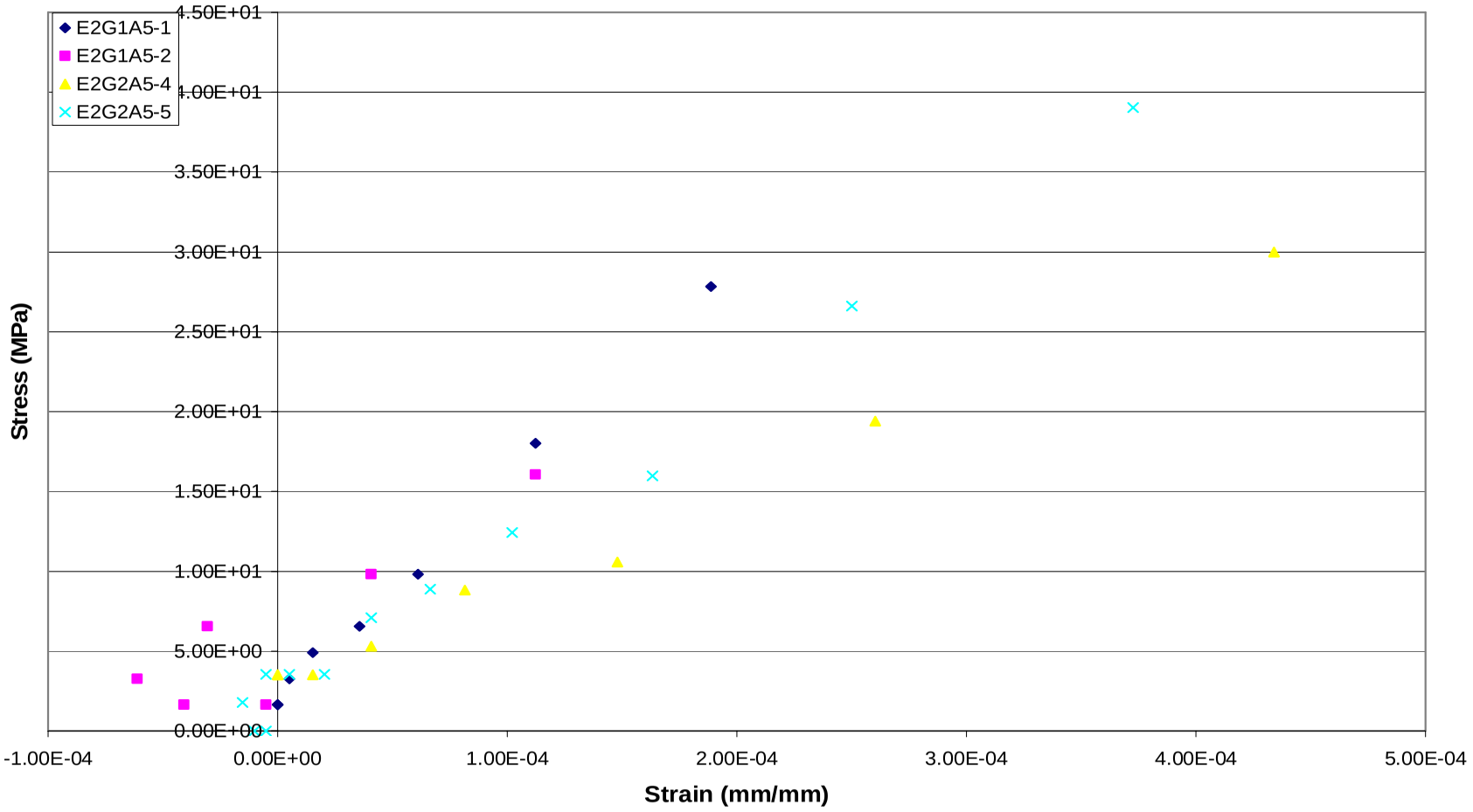

Figure 4.10 The stress – strain data for the glass reinforced tubes of $[90°]_5$ winding angle configuration.

4.2. Performance Factors

As discussed in the previous chapters, tex values for the glass and carbon reinforcements employed in this work are different with each other. This difference brings a dissimilarity in the wall thicknesses of the tubes, although the number of layers wound are similar. To fully wrap the surface of the mandrel, nearly same length of fiber is used during the production of all tubes, but as the linear density of the glass fibers is higher than that of carbon fiber, even the same number of layers of winding result in different wall thicknesses, that is, wall thicknesses of glass reinforced tubes are larger than the wall thicknesses of carbon reinforced tubes, for the same winding angle configuration. Besides, the change in winding angle configuration and extra tensioning may also lead to differences in wall thicknesses of the tubes, even if the number of layers wound are the same or similar.

The burst pressure is used to calculate the stresses on the tube, but since the burst pressure is strongly dependent on the wall thicknesses and the wall thicknesses are different for each tube, it would be better to discuss the burst pressure data in terms of the performance factor. The performance factor makes the burst pressure data independent of the effect of the wall thickness.

Performance factor, N, is determined by Equation 4.1.

$$N = PV/W \tag{4.1}$$

where
P: burst pressure, Pa
V: internal volume of the tube, m^3
W: weight of the tube, kg

The performance factors of the test tubes are given in Table 4.3. The obtained values for the performance factor are multiplied by a factor of 10^{-3}, in order to have a better visualization of the data.

Table 4.3 Burst performance factors for the test tubes.

Test Tube Number	**Test Result (bars)**	**Test Results (Pa)**	**Weight (kg)**	**Weight (N)**	**V_{in} (m^3)**	**N (1/m)**	**N*10^{-3} (1/m)**
E1 G1 A1 - 1	147	14700000	0.316	3.0968	0.00113	5365.823	5.37
E1 G1 A1 - 2	114	11400000	0.316	3.0968	0.00113	4161.25	4.16
E1 G1 A1 - 4	118	11800000	0.316	3.0968	0.00113	4307.259	4.31
E1 G2 A1 - 1	96	9600000	0.316	3.0968	0.00113	3504.211	3.50
E1 G2 A1 - 2	78	7800000	0.316	3.0968	0.00113	2847.171	2.85
E1 G2 A1 - 3	159	15900000	0.316	3.0968	0.00113	5803.849	5.80
E1 G1 A2 - 1	418	41800000	0.324	3.1752	0.00113	14881.18	14.88
E1 G1 A2 - 2	422	42200000	0.324	3.1752	0.00113	15023.58	15.02
E1 G2 A2 - 1	382	38200000	0.313	3.0674	0.00113	14077.49	14.08
E1 G2 A2 - 2	**NO FAILURE**	-	0.313	3.0674	0.00113	-	-
E1 G1 A3 - 1	**NO FAILURE**	-	0.308	3.0184	0.00113	-	-
E1 G1 A3 - 2	**NO FAILURE**	-	0.308	3.0184	0.00113	-	-
E1 G1 A3 - 3	540	54000000	0.308	3.0184	0.00113	20223.16	20.22
E1 G2 A3 - 1	498	49800000	0.308	3.0184	0.00113	18650.25	18.65
E1 G2 A3 - 2	**NO FAILURE**	-	0.308	3.0184	0.00113	-	-
E1 G1 A4 - 1	141	14100000	0.332	3.2536	0.00113	4898.771	4.90
E1 G1 A4 - 2	140	14000000	0.332	3.2536	0.00113	4864.028	4.86
E1 G2 A4 - 1	134	13400000	0.332	3.2536	0.00113	4655.569	4.66
E1 G2 A4 - 2	137	13700000	0.332	3.2536	0.00113	4759.798	4.76
E1 G1 A5 - 1	17	1700000	0.28	2.744	0.00113	700.3207	0.70
E1 G1 A5 - 2	22	2200000	0.28	2.744	0.00113	906.2974	0.91

Table 4.3 (continued)

Test Tube Number	Test Result (bars)	Test Results (Pa)	Weight (kg)	Weight (N)	V_{in} (m3)	N (1/m)	$N*10^{-3}$ (1/m)
E1 G2 A5 - 1	26	2600000	0.269	2.6362	0.00113	1114.877	1.11
E1 G2 A5 - 2	22	2200000	0.269	2.6362	0.00113	943.3579	0.94
E2 G1 A1 - 4	220	22000000	0.524	5.1352	0.00113	4842.81	4.84
E2 G1 A1 - 5	236	23600000	0.524	5.1352	0.00113	5195.015	5.20
E2 G1 A1 - 6	220	22000000	0.524	5.1352	0.00113	4842.81	4.84
E2 G2 A1 - 1	91	9100000	0.525	5.145	0.00113	1999.347	2.00
E2 G2 A1 - 2	**NO P DATA**	-	0.525	5.145	0.00113	-	-
E2 G2 A1 - 4	**NO P DATA**	-	0.528	5.1744	0.00113	-	-
E2 G2 A1 - 5	194	19400000	0.528	5.1744	0.00113	4238.126	4.24
E2 G2 A1 - 6	183	18300000	0.528	5.1744	0.00113	3997.82	4.00
E2 G1 A2 - 1	371	37100000	0.528	5.1744	0.00113	8104.87	8.10
E2 G1 A2 - 2	396	39600000	0.528	5.1744	0.00113	8651.02	8.65
E2 G2 A2 - 1	**NO FAILURE**	-	0.525	5.145	0.00113	-	-
E2 G2 A2 - 2	**NO P DATA**	-	0.525	5.145	0.00113	-	-
E2 G2 A2 - 3	274	27400000	0.525	5.145	0.00113	6020.012	6.02
E2 G2 A2 - 4	285	28500000	0.525	5.145	0.00113	6261.691	6.26
E2 G2 A2 - 5	**NO FAILURE**	-	0.525	5.145	0.00113	-	-
E2 G1 A3 - 1	**NO FAILURE**	-	0.506	4.9588	0.00113	-	-
E2 G1 A3 - 2	**NO FAILURE**	-	0.506	4.9588	0.00113	-	-
E2 G1 A3 - 4	450	45000000	0.506	4.9588	0.00113	10258.13	10.26
E2 G1 A3 - 5	425	42500000	0.506	4.9588	0.00113	9688.231	9.69
E2 G2 A3 - 1	471	47100000	0.508	4.9784	0.00113	10694.57	10.69
E2 G2 A3 - 2	457	45700000	0.508	4.9784	0.00113	10376.68	10.38
E2 G1 A4 - 4	114	11400000	0.556	5.4488	0.00113	2365.027	2.37
E2 G1 A4 - 5	120	12000000	0.556	5.4488	0.00113	2489.502	2.49
E2 G2 A4 - 4	110	11000000	0.555	5.439	0.00113	2286.156	2.29
E2 G2 A4 - 5	108	10800000	0.555	5.439	0.00113	2244.589	2.24
E2 G1 A5 - 1	17	1700000	0.476	4.6648	0.00113	411.9534	0.41

Table 4.3 (continued)

Test Tube Number	Test Result (bars)	Test Results (Pa)	Weight (kg)	Weight (N)	V_{in} (m3)	N (1/m)	$N*10^{-3}$ (1/m)
E2 G1 A5 - 2	10	1000000	0.476	4.6648	0.00113	242.3255	0.24
E2 G2 A5 - 4	17	1700000	0.483	4.7334	0.00113	405.983	0.41
E2 G2 A5 - 5	22	2200000	0.483	4.7334	0.00113	5.25E-08	0.53

4.3 Hoop Elastic Constants

During the evaluation of the stress – strain data, in order to minimize the errors that can be originated from the strain gauges, special attention is paid on the strain gauge data. The strain values that show inconsistency after a certain period of testing time are disregarded with inconsistent data recorded at the beginning of some tests. At the end of the tests, due to the very high strains formed in the tubes, which can even exceed the measurement limit of the strain gauges, some illogical data are recorded. These data are ignored as well.

Except the tubes of numbers E2G1A1 – 4, E2G1A1 – 5, E2G1A1 – 6, E2G2A1 – 5, E2G2A1 – 6, E2G1A2-1, E2G1A2 – 2, E2G2A2 – 1, E2G2A2 – 3, E2G2A2 – 4, E2G2A2 – 5, E2G1A3 – 1, E2G1A4 – 4, E2G1A4 – 5, all the stress – strain data nearly lie linear and hoop elastic constants are determined without any trouble. For the mentioned tubes, except E2G1A4 – 4, E2G1A4 – 5, the stress – strain curves display regular changes in slope with increasing pressure values. For these tubes, the first linear part of the curve is considered and evaluated to determine the hoop elastic modulus. The reason for the difference in slopes and the resulting data will be discussed in the following chapter. For the tubes of numbers E2G1A4 – 4, E2G1A4 – 5, the stress – strain data are rather unusual, and special attention will be paid for their evaluation. The hoop elastic constants for the test tubes are given in Table 4.4.

Table 4.4. Hoop elastic constants for the tubes.

Test Tube Number	Test Result (bars)	E (GPa)
E1 G1 A1 - 1	147	20.9
E1 G1 A1 - 2	114	19.98
E1 G1 A1 - 4	118	17.35
E1 G2 A1 - 1	96	22.35
E1 G2 A1 - 2	78	18.93
E1 G2 A1 - 3	159	22.98
E1 G1 A2 - 1	418	49.54
E1 G1 A2 - 2	422	54.71
E1 G2 A2 - 1	382	47.84
E1 G2 A2 - 2	NO FAILURE	47.21
E1 G1 A3 - 1	NO FAILURE	113.24
E1 G1 A3 - 2	NO FAILURE	120.39
E1 G1 A3 - 3	540	115.7
E1 G2 A3 - 1	498	961.45
E1 G2 A3 - 2	NO FAILURE	98.261
E1 G1 A4 - 1	141	166.36
E1 G1 A4 - 2	140	299.42
E1 G2 A4 - 1	134	199.873
E1 G2 A4 - 2	137	280.58
E1 G1 A5 - 1	17	29.89
E1 G1 A5 - 2	22	39.46
E1 G2 A5 - 1	26	284.16
E1 G2 A5 - 2	22	25.29
E2 G1 A1 - 4	220	37.82
E2 G1 A1 - 5	236	37.32
E2 G1 A1 - 6	220	27.94
E2 G2 A1 - 1	91	20.97
E2 G2 A1 - 2	**NO P DATA**	-

Table 4.4 (continued)

Test Tube Number	Test Result (bars)	E (GPa)
E2 G2 A1 - 4	**NO P DATA**	-
E2 G2 A1 - 5	194	32.3
E2 G2 A1 - 6	183	17.82
E2 G1 A2 - 1	371	41.36
E2 G1 A2 - 2	396	37.46
E2 G2 A2 - 1	NO FAILURE	33.69
E2 G2 A2 - 2	**NO P DATA**	-
E2 G2 A2 - 3	274	22.33
E2 G2 A2 - 4	285	40.26
E2 G2 A2 - 5	NO FAILURE	19.81
E2 G1 A3 - 1	NO FAILURE	86.04
E2 G1 A3 - 2	NO FAILURE	49.02
E2 G1 A3 - 4	**450** **NO P DATA**	-
E2 G1 A3 - 5	425	53.12
E2 G2 A3 - 1	471	39.06
E2 G2 A3 - 2	457	52.31
E2 G1 A4 - 4	114	84.83
E2 G1 A4 - 5	120	78.24
E2 G2 A4 - 4	110	154.68
E2 G2 A4 - 5	108	92.72
E2 G1 A5 - 1	17	135.28
E2 G1 A5 - 2	10	69.76
E2 G2 A5 - 4	17	64.04
E2 G2 A5 - 5	22	88.83

As can be observed from the Table 5.1, hoop elastic constant values for the tubes E1 G2 A3 – 1, E1 G1 A4 – 2, E1 G2 A4 – 1, E1 G2 A4 – 2, E1 G2 A5 – 1, E2 G2 A4 – 4 and E2 G1 A5 – 1 are extremely high. Their irrationally high values are probably due to some experimental errors originating from the strain gauge measurements. Their evaluated hoop elastic modulus data will be ignored in discussions.

CHAPTER V

DISCUSSIONS

5.1. Burst Pressure Studies

In this section, the burst performance of the filament wound tubes are discussed, and the effects of the process parameters (fiber type, extra tensioning for the fibers and winding angle configuration) on the performance, is explained. As discussed in the previous chapter, performance factors will be used in order to form a reliable basis for comparison of data. Burst performance factor values are determined by taking the average data from the tubes made of the same matrix and reinforcement, and of the same winding angle configurations.

5.1.1 Effect of Winding Angle Configuration

Winding angle dependence of the burst pressure of the test tubes is discussed in terms of burst performance factors. Figure 5.1 and 5.2 present the change in burst performance factor of the carbon fiber reinforced tubes without and with extra tensioning, respectively.

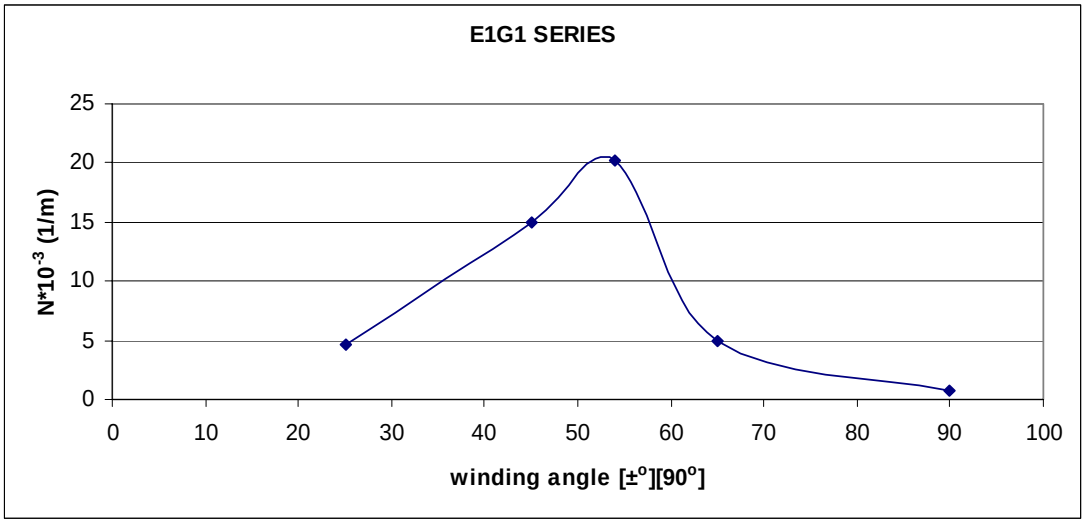

Figure 5.1. Burst performance factors for the carbon fiber reinforced tubes manufactured without extra tensioning.

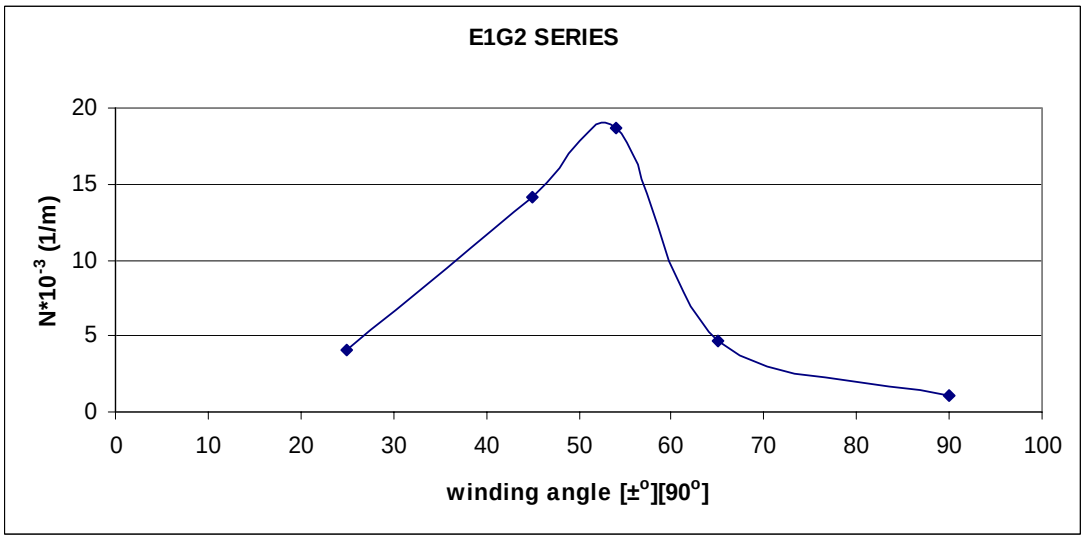

Figure 5.2. Burst performance factors for the carbon fiber reinforced tubes manufactured with extra tensioning.

Figure 5.3 and 5.4 presents the change in burst performance factor of the glass fiber reinforced tubes with and without tensioning, respectively.

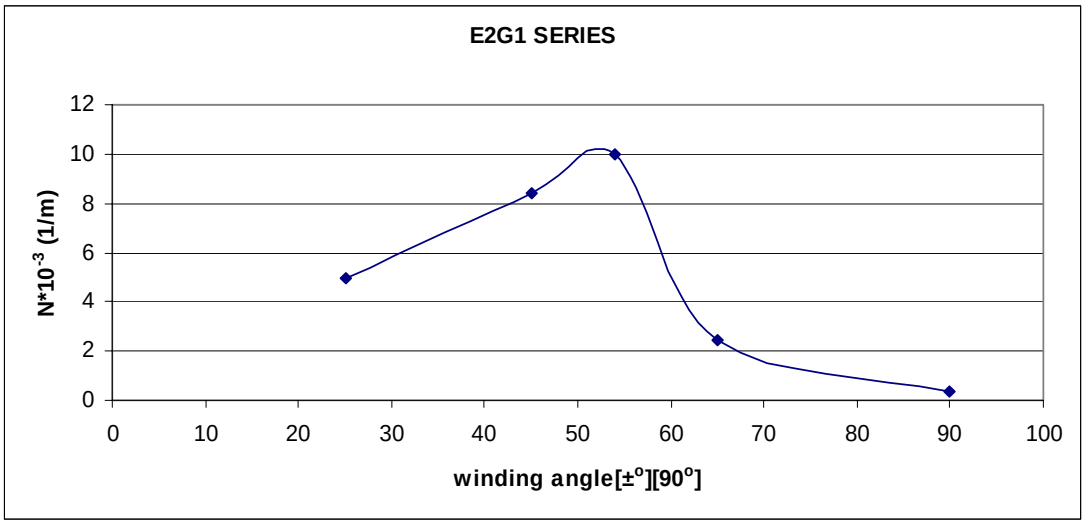

Figure 5.3. Burst performance factors for the glass fiber reinforced tubes manufactured without extra tensioning.

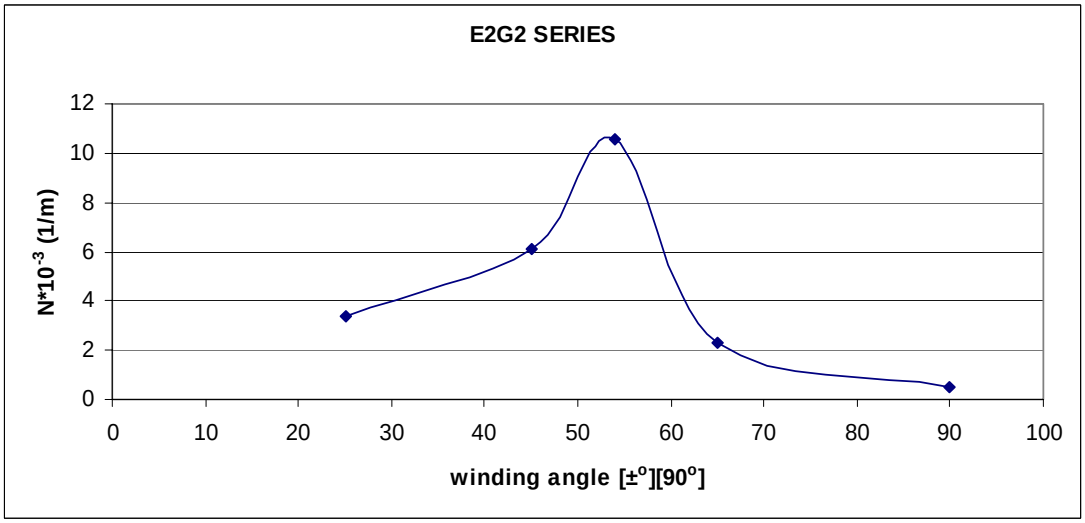

Figure 5.4. Burst performance factors for the glass fiber reinforced tubes manufactured with extra tensioning.

It can be observed from the Figures 5.1, 5.2, 5.3 and 5.4 that under internal pressure, the burst pressure performance increases with increasing winding angle configuration, reaches to maximum at the winding angle configuration of [±54°][90°] for both fiber types and tensioning conditions, and for larger winding configurations than [±54°][90°], the burst pressure performance decreases. The variation in the burst performance with changing winding angle configuration is expected, as the composite materials show an anisotropic behavior under different loading conditions. Being highly anisotropic, when loaded in the direction of the fiber alignment, composite materials are likely to exhibit the best mechanical properties. For hoop loading condition, as the winding angle increases, the fiber alignment direction becomes closer to the loading direction, and for [90°] winding configuration, where the loading direction is the same as fiber alignment direction, it shall show a maximum. On the other hand, as the winding angle increases, the resistance of the composite tube to axial load decreases. The hoop layer present as the outermost layer of all the tubes increases the hoop strength significantly, but it has a very low resistance to axial loads. Internal pressure loading is a combined loading type, it creates both axial and hoop stresses in the material, and thus the maximum performance is expected to be attained in the winding configuration which optimizes the resistances to hoop and axial stresses. The increase in the burst performance of the test tubes with increasing winding angle configuration is thus expected, and can be explained by higher hoop resistances being dominant over lower axial resistances as the winding angle configuration increases. After the maximum, the detected decrease can be said to be due to the dominant lowering in axial mechanical resistance over increasing hoop resistance. Considering this, [±54°][90°] being the best winding configuration is an expected result, as it can be verified from the several data in literature [27, 28].

5.1.2 Effect of Extra Fiber Tensioning

Tension setting dependence of the burst pressure of the test tubes is also discussed in terms of burst performance factors. The effect of extra tensioning on burst

performance factors of the carbon fiber reinforced and glass fiber reinforced tubes can be observed from Figure 5.5 and 5.6, respectively.

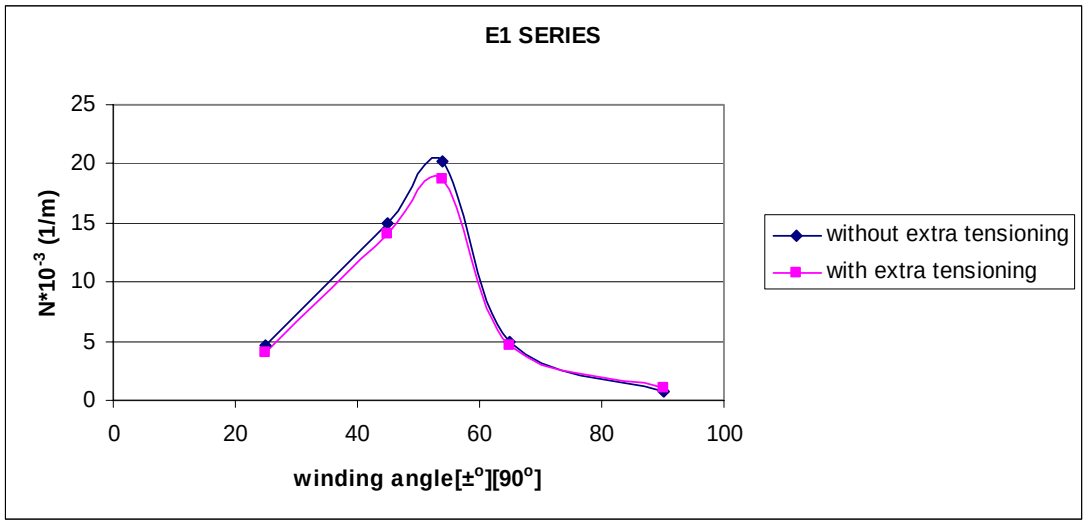

Figure 5.5. Burst performance factors for the carbon fiber reinforced tubes.

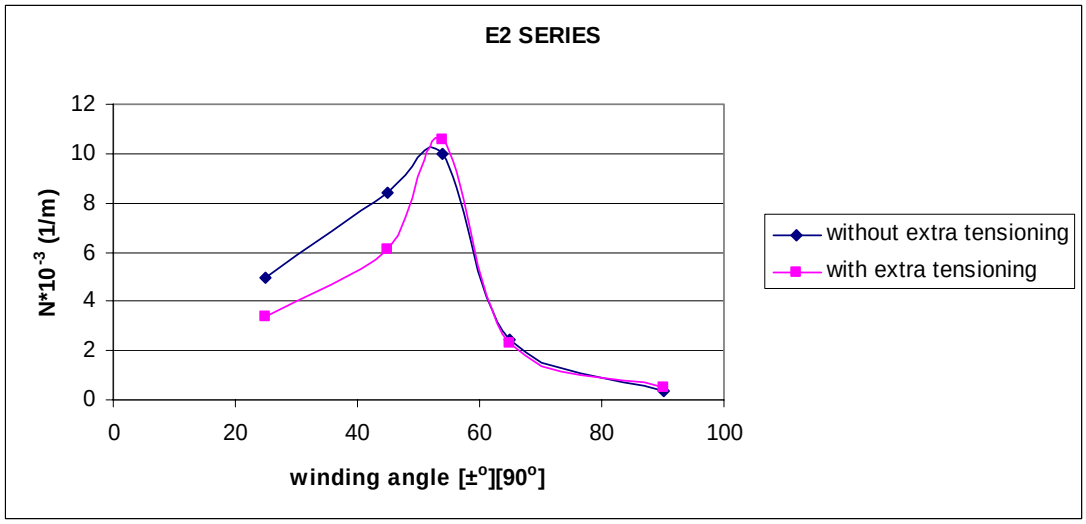

Figure 5.6 Burst performance factors for the glass fiber reinforced tubes.

Examining the figures, it can be seen that for carbon fiber reinforced tubes, the effect of extra tensioning is not significant, that is, the performance factor values for both tension settings lie in the same range for every winding angle. For glass fiber reinforced tubes, although extra tensioning seems to decrease the performance factors for the winding angles lower than [±54°][90°], it can be said that the decrease in the [±45°][90°] winding configuration burst pressure is probably due to another reason discussed in the previous chapter. The lower burst pressure data of those tubes that are subjected to excessive grinding of the tube surface for the fixing of the strain gauges resulted in the loss of a part of the outermost layer of the tubes. During the tests, it was observed that the failure started at these regions where an excessive grinding was present and the burst pressures are quite lower than expected. An evidence for that is that a similar tube that belongs to the same parent tube withstood an internal pressure of 359 bar without failure, whose performance factor could not be evaluated because a successful catastrophic failure could not be obtained. For the winding angles above [±54°][90°], the effect of extra tensioning is not significant, and extra tensioning need not necessarily be considered while optimizing the process parameters for maximum burst performance.

5.1.3 Effect of the Type of Reinforcement Material

Fiber type is another production parameter considered in this work. The burst performance of the two types of the fibers used can be seen in Figures 5.7 and 5.8 for the tubes manufactures without extra tensioning and with extra tensioning, respectively.

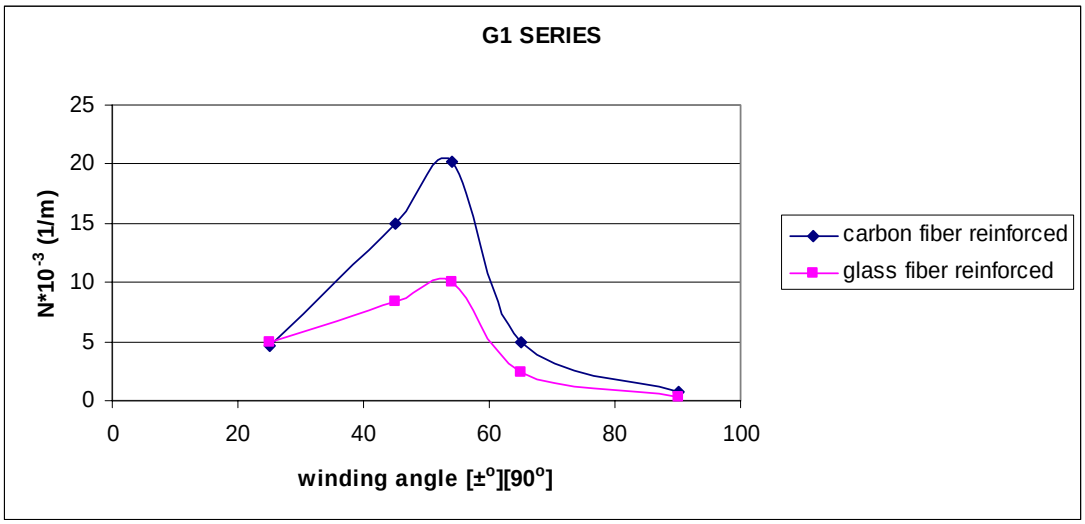

Figure 5.7 Burst performance factors of the tubes without extra tensioning.

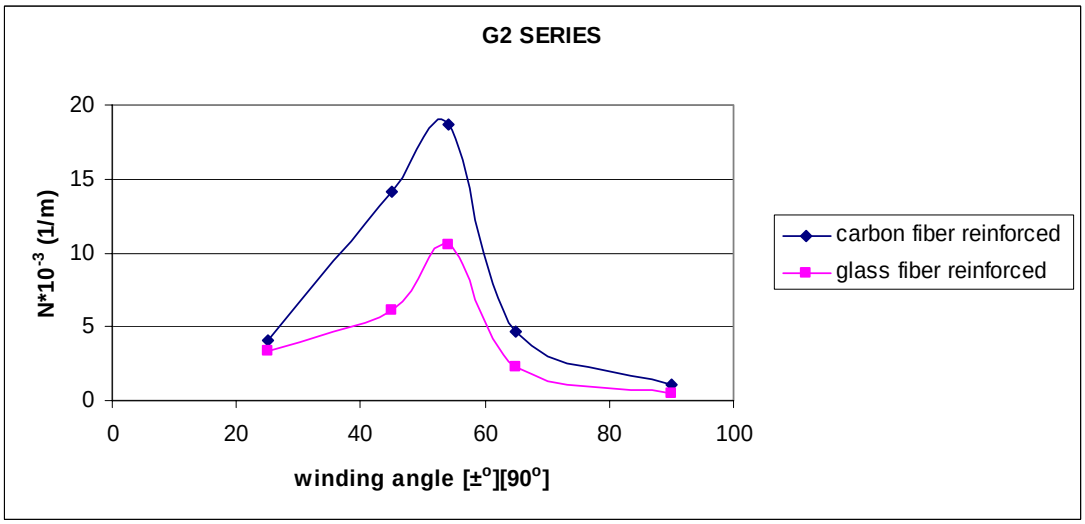

Figure 5.8 Burst performance factors of the tubes with extra tensioning.

Examining the figures, it can be seen that carbon fiber reinforced tubes show a much better burst performance compared to the glass fiber reinforced ones. This is an expected result considering that carbon fibers are much stronger and stiffer than the glass fibers.

An overall look at the burst pressure performance factors is given in Figure 5.9.

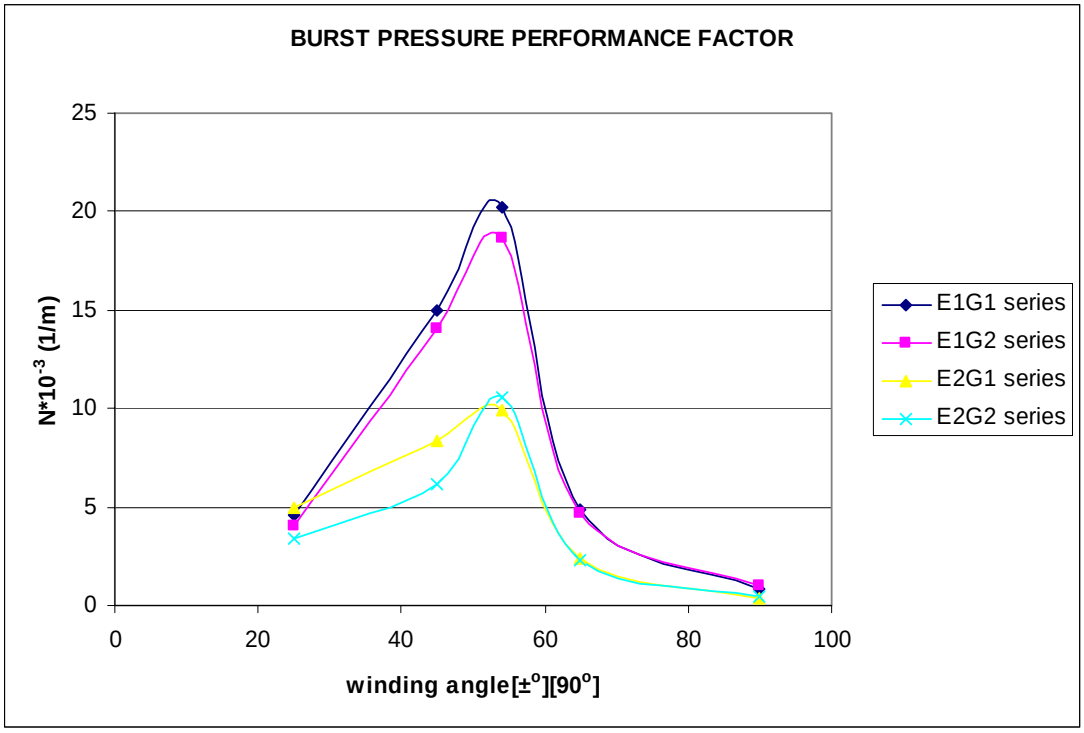

Figure 5.9 Burst pressure performance factors.

As a result, considering the test results, when the burst pressure performance is of primary importance for the filament wound tubes, it can be said that carbon fiber reinforced tubes with the winding configuration of [±54°][90°], shall be the best choice for such internal pressure applications. Extra tensioning is observed not to have a significant effect on burst pressure performance.

5.2 Hoop Elastic Constant Studies

This section will discuss the hoop elastic constants of the filament wound tubes, obtained by evaluating the hoop stress – strain data presented in the previous chapter. The effects of winding angle configuration, extra tensioning for fibers and the fiber type will also be discussed.

5.2.1 Effect of Winding Angle Configuration

In Figure 5.10 and 5.11, the changes in the hoop elastic constants of the carbon fiber reinforced tubes, manufactured with different winding angles are compared for the tubes manufactured without and with extra tensioning, respectively.

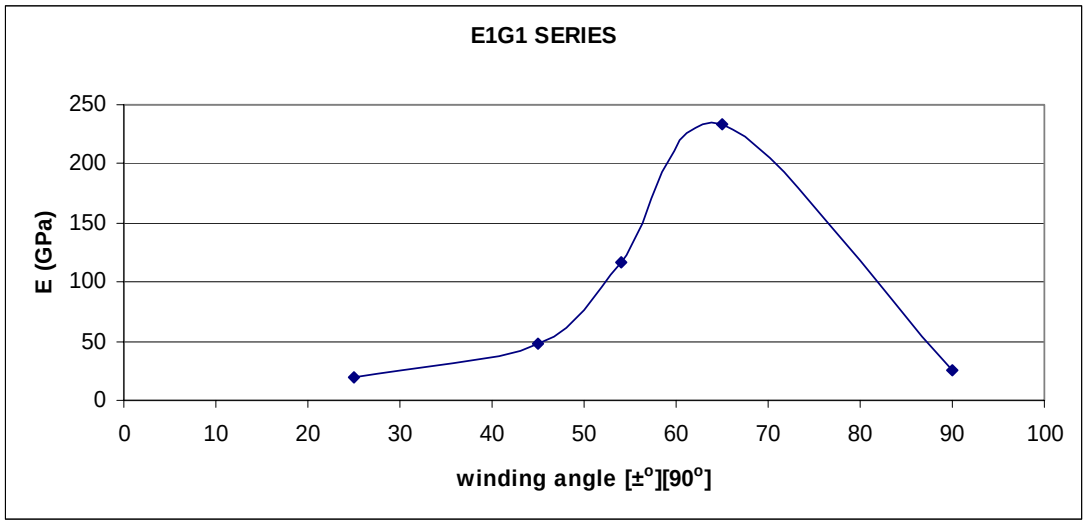

Figure 5.10 Hoop elastic constant of the carbon fiber reinforced tubes manufactured without extra tensioning.

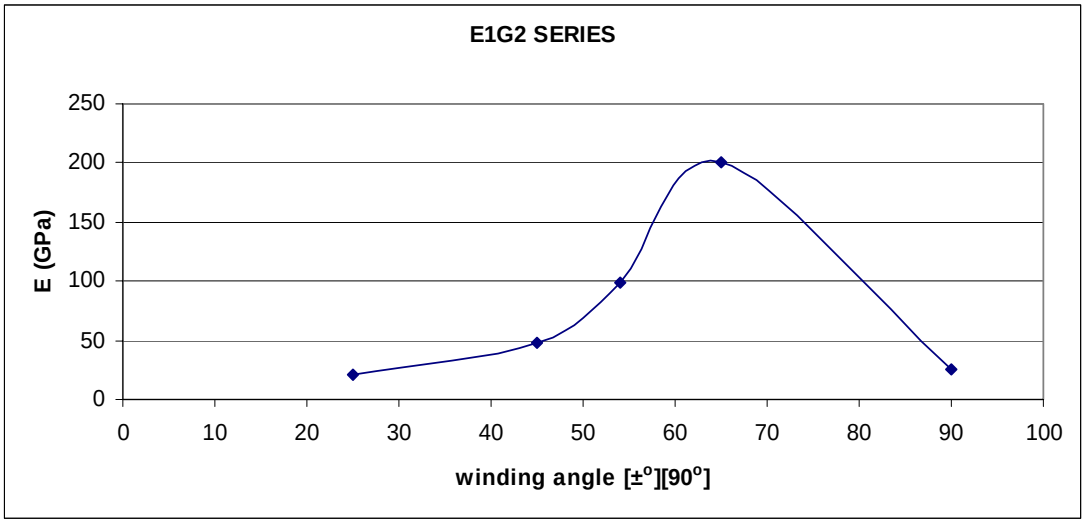

Figure 5.11 Hoop elastic constant of the carbon fiber reinforced tubes manufactured with extra tensioning.

Figures 5.12 and 5.13 present the change in hoop elastic constants of the glass fiber reinforced tubes with and without tensioning, respectively.

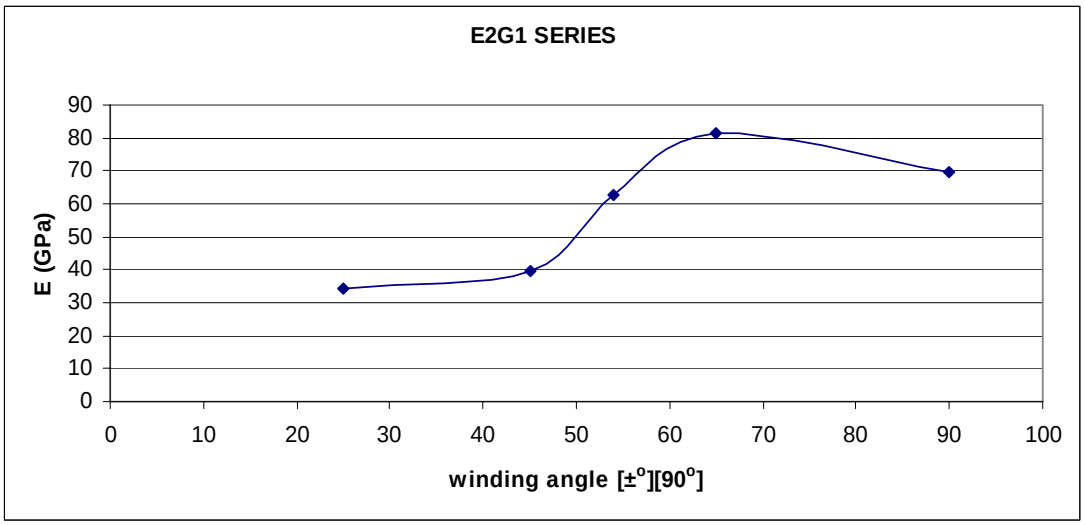

Figure 5.12 Hoop elastic constant of the glass fiber reinforced tubes manufactured without extra tensioning.

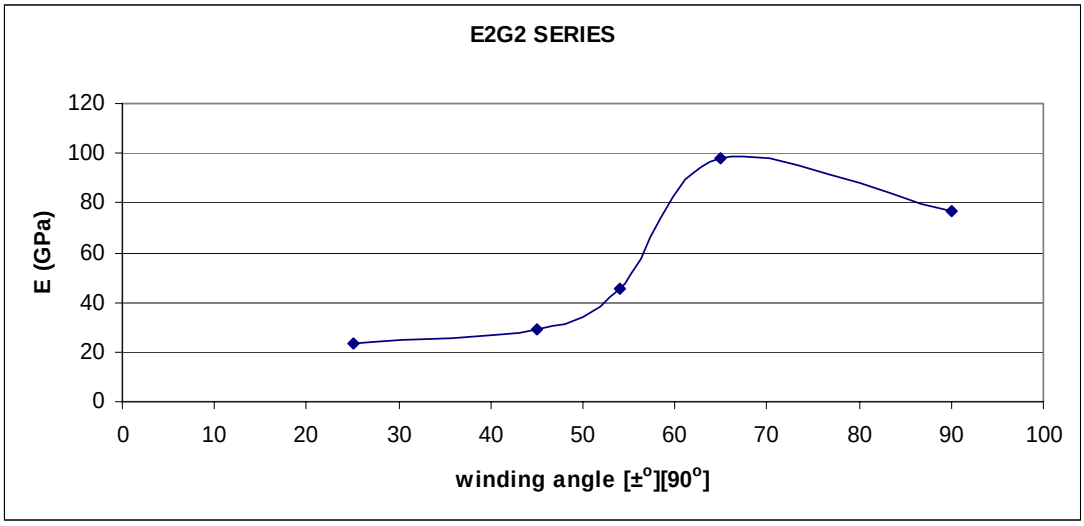

Figure 5.13 Hoop elastic constant of the glass fiber reinforced tubes manufactured with extra tensioning.

It is seen from the figures that for both fiber types and extra tensioning conditions, the hoop elastic constants increase with the increasing winding angle configuration, reaching to maximum at the winding angle configuration of [±65°][90°], and decreases for greater winding configurations, [90°]. Like the burst pressure performance, this behavior can be related to the anisotropic behavior of the composites. The elastic constants and stiffness values for the composites when loaded in their fiber alignment condition, exhibit a maximum and as the winding angle decreases, the elastic constant in the hoop loading direction also decreases. For the configuration of [±65°][90°], the resistance to loading in hoop direction is so large that the tube expands in axial direction much more than it does in hoop direction. As a result of this, the strain gauges give lower deformations and thus higher hoop elastic constant compared to the tensile elastic constant in fiber direction, E_{11}. For the configuration of [90°], the expansion in hoop direction is very hard and limited, and the tube would like to expand in axial direction instead. But, due to the very low pressure resistance of the configuration in axial direction, it cannot elongate in axial direction and so it cannot decrease the expansion in hoop

direction as it fails very quickly due to the axial loads. As a result, the elastic constant of [90°] winding angle configuration is lower than expected.

5.2.2 Effect of Extra Fiber Tensioning

The effect of extra tensioning on burst performance factors of the carbon fiber reinforced and glass fiber reinforced tubes can be observed from Figure 5.14 and 5.15, respectively.

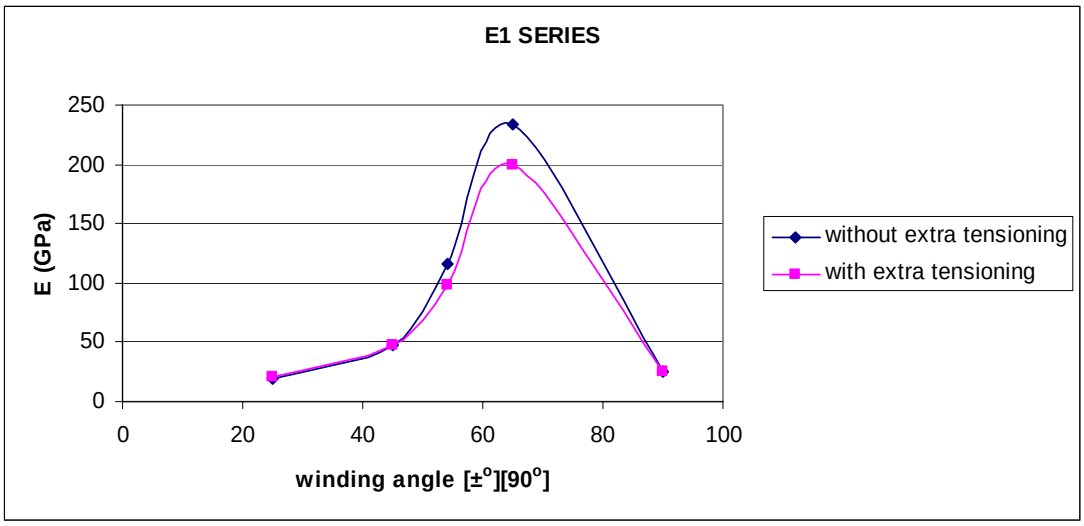

Figure 5.14 Hoop elastic constants of the carbon fiber reinforced tubes.

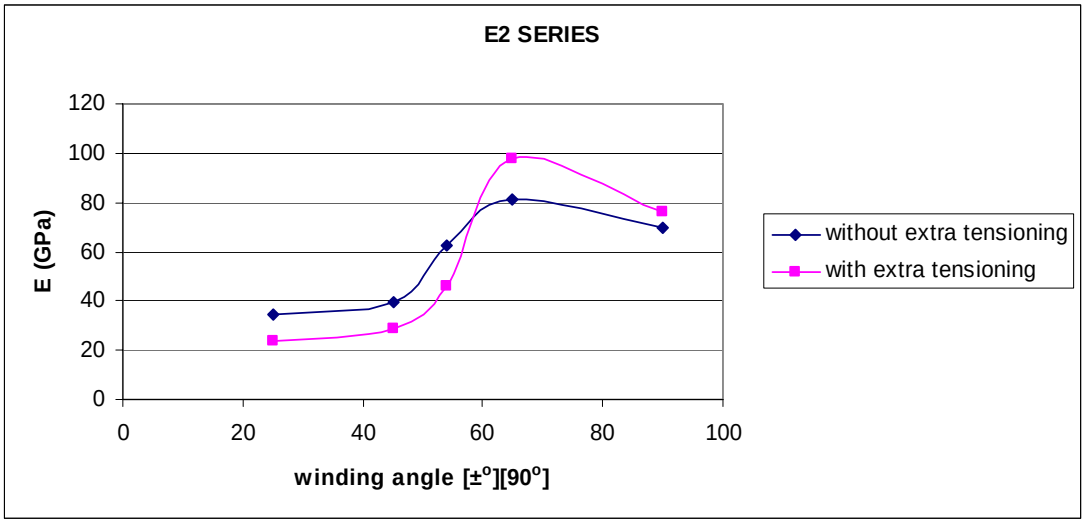

Figure 5.15 Hoop elastic constants of the glass fiber reinforced tubes.

Examining the figures, it can be seen that for carbon fiber reinforced tubes, the effect of extra tensioning is not significant on the hoop elastic constant values, that is, the hoop elastic constant values for both tension settings lie in the same range for every winding angle. On the other hand, for glass fiber reinforced tubes, extra tensioning seems to increase the hoop elastic constant considerably for the [±65°][90°] winding configuration. This unexpected increase is probably due to unusual stress – strain data exhibited by glass fiber reinforced tubes produced by this winding configuration, which is given in the previous chapter. The strain response of the tube to internal pressure load is very limited in the first part of loading, and it exhibits very low strains that results in hoop elastic constants even higher than that of single glass fiber. During the test, it was observed that the failure mode of the [±65°][90°] tubes are quite different than expected as well, which, will be discussed in the following section. The first part of the stress – strain curve has a very high slope as mentioned, and once the failure begins, the strain response changes and the strains formed in the tube increase with the increasing load, which results in a lower slope and thus hoop elastic constant. This failure can be observed during the test as formation of subsections at the tube that move free from each other, which will also

be discussed in the following section. Other than that, considering the figures, it can be said that the effect of extra tensioning is not significant, and extra tensioning need not necessarily be considered while optimizing the process parameters for maximum burst performance. It follows that extra tensioning does not in any case increase the fiber wetting and so does not affect the bonding.

5.2.3 Effect of the Type of Reinforcement Material

The hoop elastic constants of the two types of the fibers used are presented in Figures 5.16 and 5.17 for the tubes manufactured without extra tensioning and with extra tensioning, respectively.

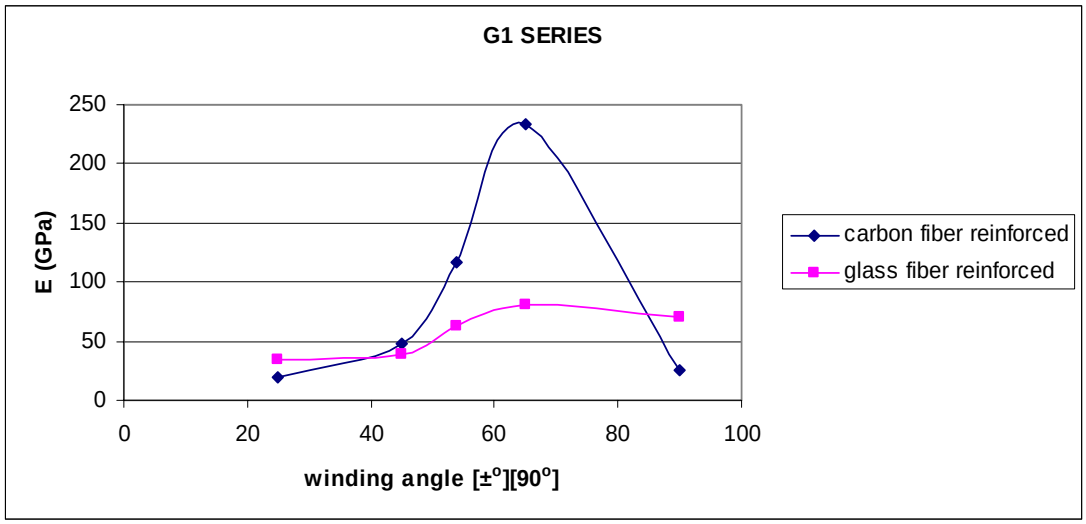

Figure 5.16 Hoop elastic constants of the tubes without extra tensioning.

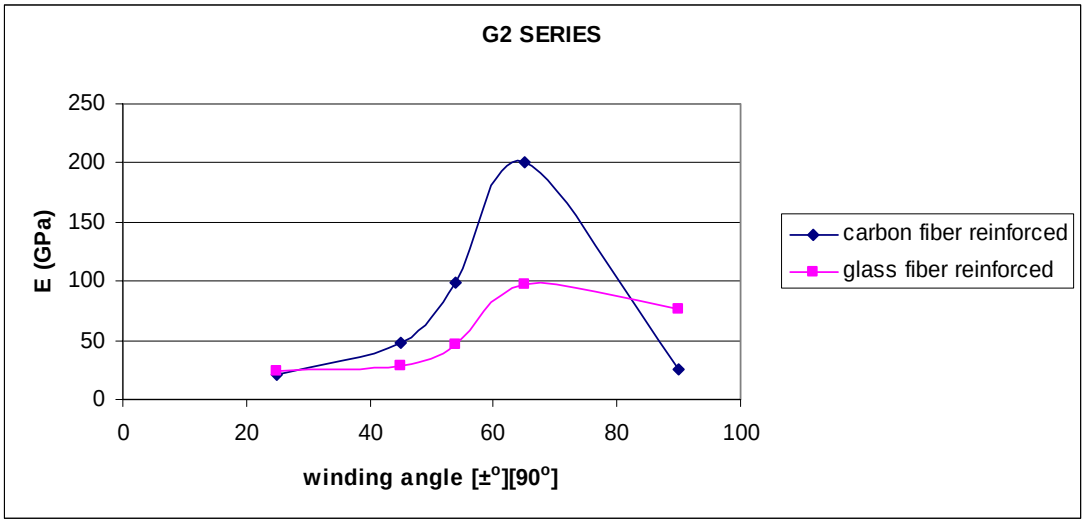

Figure 5.17 Hoop elastic constants of the tubes with extra tensioning.

Examining the figures, it can be seen that carbon fiber reinforced tubes exhibit a much larger hoop elastic constants compared to the glass fiber reinforced ones. The increase in the hoop elastic constant with increasing angle before reaching to a maximum becomes much significant for the carbon reinforced tubes. This is an expected result considering that carbon fibers are much more anisotropic; are stronger and stiffer than the glass fibers in the hoop loading direction but the degradation of the mechanical properties of the carbon fiber reinforced structures becomes more pronounceable for the lower winding angles.

An overall look at the hoop elastic constants is given in Figure 5.18.

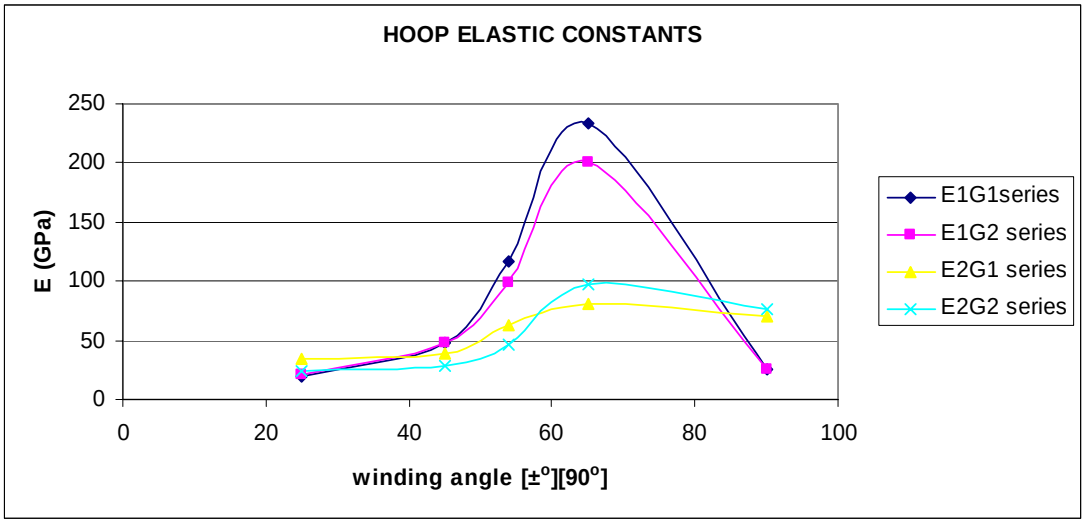

Figure 5.18 Hoop elastic constants.

Considering the test results, when the high hoop elastic constant is of primary importance for the filament wound tubes, it can be said that carbon fiber reinforced tubes with the winding configuration of [±65°][90°], shall be the best choice for such internal pressure applications. Extra tensioning is again observed not to have a significant effect on burst pressure performance.

5.3 Failure Modes

As discussed in the previous chapters, the failure in the tests are required to be catastrophic, that is, bursting is desired. In order to assure catastrophic failure, elastomeric internal liners are placed in the test tubes, which are to prevent any leakage from the possible matrix cracks and accordingly avoid a decrease in the internal pressure before catastrophic failure occurs.

During the experiments, the failure modes that can be seen are ply failures that take place in the outermost layer and simple catastrophic failures, where all the layers fail at the same time. Any ply failure that originates in the inner layers, but not the

outermost layer cannot be observed during experiment, but can be figured out from the evaluation of the stress – strain data.

For the winding configuration of $[\pm 25°]_3$ $[90°]_1$, carbon reinforced tubes except E1G2A1-1, exhibit a regular stress – strain data, that is, no considerable change is slope is observed and the curve is almost linear until failure. This implies that the failure that occurred may simply be catastrophic, that is, all the layers have failed at the same time. Another possibility is that first ply failure has taken place first, and the time interval between the first ply failure and final failure is so short that the recording speed of the strain gauge data acquisition system was unable to detect that possible ply failure, and indicate it in the stress – strain curve. An example of a failed carbon fiber reinforced tube of $[\pm 25°]_3$ $[90°]_1$ winding configuration is given in Figure 5.19. For the glass fiber reinforced tubes of $[\pm 25°]_2$ $[90°]_1$ winding configuration, significant changes in the slopes of the stress – strain curves are observed. These changes form multiple elastic constant values in the tube at different loading times. The reason for that change is probably ply failures of inner layers. In a laminate, each ply tends to perform as though itself and when one of the plies in the structure starts to fail, it cracks the matrix around and there appears an increase in the strain and thus the slope decreases. When the first ply failure is completed, the structure starts to behave in its original way, as one ply is completely gone and other plies stand intact. The strain response of the tube is restored but the load carrying thickness of the tube is decreased due to the failure of one of the layers. As the wall thickness of the tube is decreased, it cannot carry more load anymore, and fails. The second and third slope values are the hoop elastic constant values for damaged tubes and are not considered in this work. The reason is that this work aims to produce data for the design applications and the structures are generally designed without failure condition. An example of the failed glass fiber reinforced tube of $[\pm 25°]_2$ $[90°]_1$ winding configuration is given in Figure 5.20.

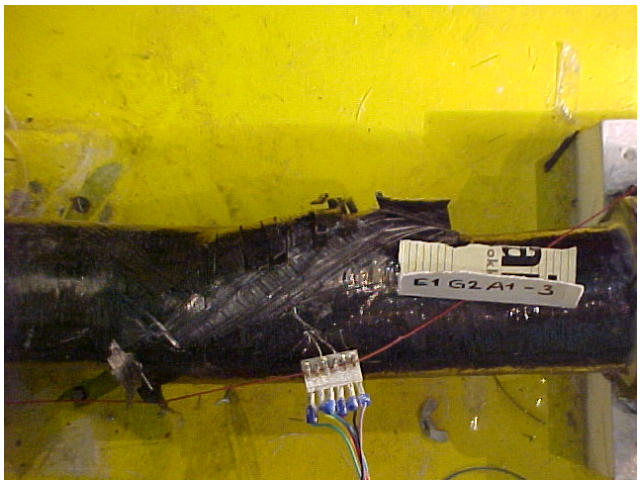

Figure 5.19. Failed carbon fiber reinforced tube of $[\pm 25°]_3\,[90°]_1$ winding configuration.

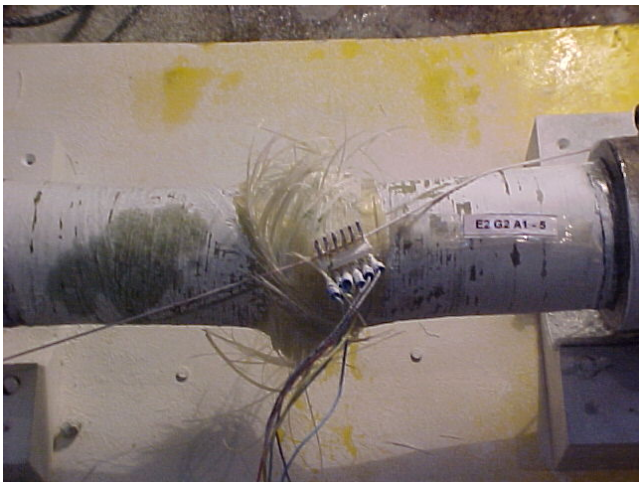

Figure 5.20. Failed glass fiber reinforced tube of $[\pm 25°]_2\,[90°]_1$ winding configuration.

For the winding configuration of $[\pm 45°]_3\,[90°]_1$, carbon reinforced tubes exhibit a regular stress – strain data, but some slight change in slopes are observed just before failure. These changes are due to the first ply failures in the structure, and after the first ply failure, the structure could not carry more load and failed catastrophically.

An example of a failed carbon fiber reinforced tube of $[\pm 45°]_3$ $[90°]_1$ winding configuration is given in Figure 5.21. For the glass fiber reinforced tubes of the $[\pm 45°]_2$ $[90°]_1$ winding configuration, significant changes in the slopes of the stress – strain curves are observed. The reason for that change is probably the first ply failures, and for the tube number E2G2A2-3, the stress – strain data implies multiple changes in slope, that is, several ply failures. An example of the failed glass fiber reinforced tube of $[\pm 45°]_2$ $[90°]_1$ winding configuration is given in Figure 5.22.

Figure 5.21. Failed carbon fiber reinforced tube of $[\pm 45°]_3$ $[90°]_1$ winding configuration.

Figure 5.22. Failed glass fiber reinforced tube of $[\pm 45°]_2\,[90°]_1$ winding configuration.

For the winding configuration of $[\pm 54°]_3\,[90°]_1$, carbon reinforced tubes exhibit some slight changes in slopes before failure. These changes are again due to the first ply failures in the structure, and after the first ply failure, the structure could not carry the high load and failed catastrophically. For the glass fiber reinforced tubes of the $[\pm 54°]_2\,[90°]_1$ winding configuration, significant multiple changes in the slopes of the stress – strain curves are observed, that is, several ply failures have taken place. An example of the failed glass fiber reinforced tube of $[\pm 54°]_2\,[90°]_1$ winding configuration is given in Figure 5.23.

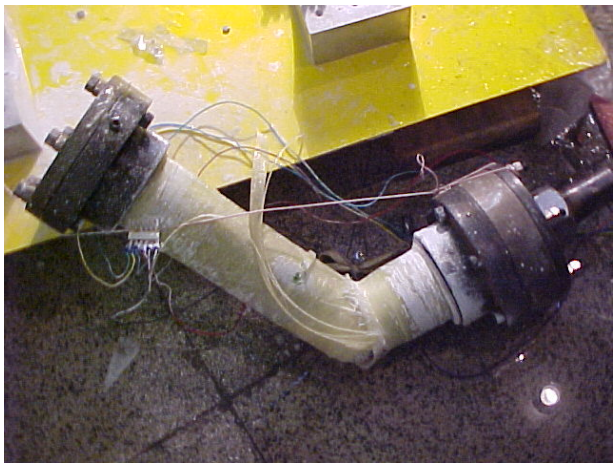

Figure 5.23. Failed glass fiber reinforced tube of $[\pm 54°]_2\,[90°]_1$ winding configuration.

For the winding configuration of $[\pm 65°]_3\,[90°]_1$, carbon reinforced tubes exhibit slight changes in slopes before failure, which implies that first ply failure takes place in the structure before the final failure. The final failure is catastrophic, and an example of a failed carbon fiber reinforced tube of $[\pm 65°]_3\,[90°]_1$ winding configuration is given in Figure 5.24. For the glass reinforced tubes of the same winding configuration, during the internal pressure tests, a different type of failure is observed. The tubes display an unusual, non-linear stress – strain curve. At the end of the test, tube loses its integrity and subsections are formed, which, makes the outer lining of the tube attain a wavy-like external appearance, but the internal pressure is still not decreased and the tube has not failed yet although buckling has occurred and subsections are formed. The reason for that appearance may be the failure of an interior layer or layers, and thus falling apart of the structure, but remembering that there lies an elastomeric liner inside, which holds the structure together, some subsections are formed in the tube. Those subsections then start to behave almost free from each other and wavy-like external appearance is observed. In other words, winding configuration is comparably weak in axial direction and the tube cannot carry more load, and the structure failed from the weak points and the tube started to behave as if it was formed of free cylinders. After the formation of subsections, the

strain response of the structure changed as given in Figure 4.9. Thus, the sudden decrease in the strains can probably be explained by the failure of one of the interior layers and formation of subsections. These subsections can move in a less restricted manner and this decreases the strain formed in the material. This failure mode can be observed from the Figure 5.25.

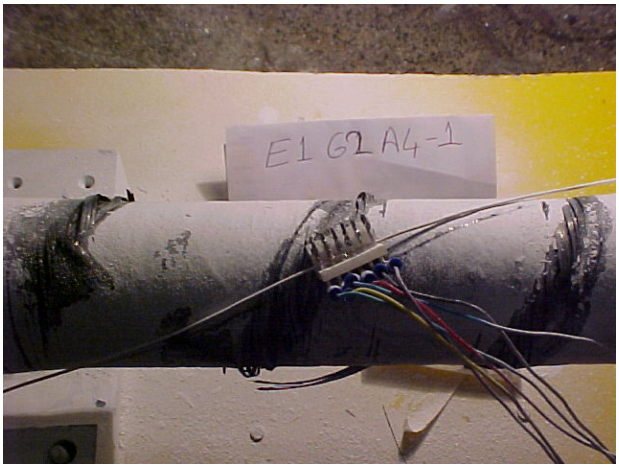

Figure 5.24. Failed carbon fiber reinforced tube of $[\pm 65°]_3\,[90°]_1$ winding configuration

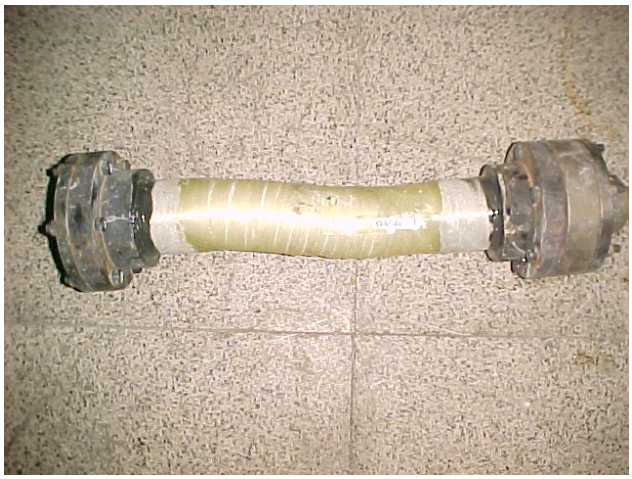

Figure 5.25. Failed glass fiber reinforced tube of $[\pm 65°]_3\,[90°]_1$ winding configuration.

When the stress – strain data of the winding configuration of [90°] for carbon fiber reinforced tubes are explored, the first point that calls attention is very low failure pressures. The tubes simply fail in axial direction. The reason is that while the tubes are extremely strong and stiff in their hoop direction, when internal loading starts, the load finds a great resistance in hoop direction. Instead, strains in axial weak directions become dominant. The structure cannot withstand more axial load and fails in a short time interval, at low internal pressures. An example of a failed glass reinforced tube of $[90°]_7$ winding angle configuration is given in Figures 5.26

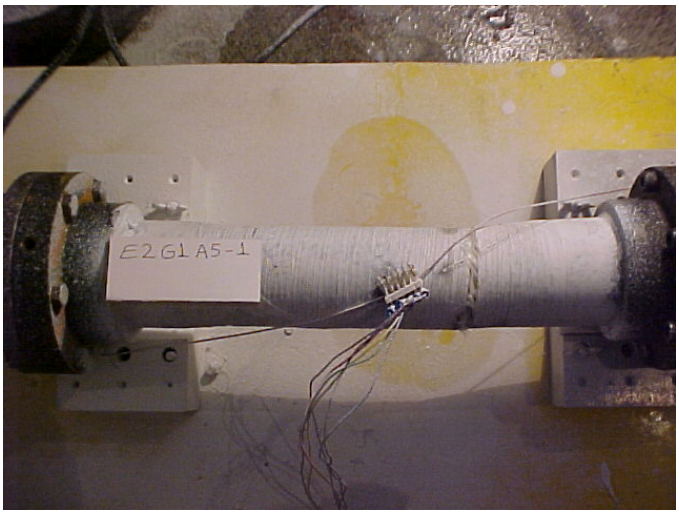

Figure 5.26. Failed glass fiber reinforced tube of $[90°]_5$ winding configuration.

5.4 Comparison of the Burst Pressure Data with Laminate Analysis

A typical filament wound laminate consists of several plies oriented at arbitrary angles and stacking sequence. In a laminate, each ply tends to perform as though by itself, but behavior of each ply is modified to interact with the remaining plies of the laminate. This interaction between the plies is important in composite laminate performance and it affects the mechanical behavior. Laminate analysis is an important tool in predicting the mechanical performance of the composite laminates.

In this study, "ASME Boiler and Pressure Vessel Code, Section X: Fiber-Reinforced Plastic Pressure Vessels" is employed for the laminate analysis for the composite tubes. Winding angle configuration, fiber and resin properties, number of layers and wall thicknesses are the inputs, and the code evaluates and returns the burst pressure and the first layer where the failure initiates. The results of the analysis are presented with the experimental results in Table 5.1.

Table 5.1 Internal pressure test and ASME Boiler and Pressure Vessel Code, Section X analysis results.

Test Tube Number	**Internal Pressure Test Results (bars)**	**ASME Section X Results (bars)**	**ASME Section X Failure Layer**
E1 G1 A1 - 1	147	90	inner layer
E1 G1 A1 - 2	114		
E1 G1 A1 - 4	118		
E1 G2 A1 - 1	96	80	inner layer
E1 G2 A1 - 2	78		
E1 G2 A1 - 3	159		
E1 G1 A2 - 1	418	390	inner layer
E1 G1 A2 - 2	422		
E1 G2 A2 - 1	382	385	inner layer
E1 G2 A2 - 2	**NO FAILURE**		
E1 G1 A3 - 1	**NO FAILURE**	390	outermost layer
E1 G1 A3 - 2	**NO FAILURE**		
E1 G1 A3 - 3	540		
E1 G2 A3 - 1	498	390	inner layer
E1 G2 A3 - 2	**NO FAILURE**		
E1 G1 A4 - 1	141	135-155	outermost layer
E1 G1 A4 - 2	140		
E1 G2 A4 - 1	134	135 - 155	outermost layer
E1 G2 A4 - 2	137		

Table 5.1 (continued)

Test Tube Number	Internal Pressure Test Results (bars)	ASME Section X Results (bars)	ASME Section X Failure Layer
E1 G1 A5 - 1	17	55-60	all layers
E1 G1 A5 - 2	22		
E1 G2 A5 - 1	26	55-60	all layers
E1 G2 A5 - 2	22		
E2 G1 A1 - 4	220	225	inner layer
E2 G1 A1 - 5	236		
E2 G1 A1 - 6	220		
E2 G2 A1 - 1	91	225	inner layer
E2 G2 A1 - 2	**NO PRESSURE DATA**		
E2 G2 A1 - 4	NO P		
E2 G2 A1 - 5	194		
E2 G2 A1 - 6	183		
E2 G1 A2 - 1	371	375	inner layer
E2 G1 A2 - 2	396		
E2 G2 A2 - 1	**NO FAILURE**	370	inner layer
E2 G2 A2 - 2	**NO PRESSURE DATA**		
E2 G2 A2 - 3	274		
E2 G2 A2 - 4	**285**		
E2 G2 A2 - 5	**NO FAILURE**		
E2 G1 A3 - 1	**NO FAILURE**	450	inner layer
E2 G1 A3 - 2	**NO FAILURE**		
E2 G1 A3 - 4	450		
E2 G1 A3 - 5	425		
E2 G2 A3 - 1	471	445	inner layer
E2 G2 A3 - 2	457		
E2 G1 A4 - 4	114	105	inner layer
E2 G1 A4 - 5	120		
E2 G2 A4 - 4	110	105	inner layer
E2 G2 A4 - 5	108		

Table 5.1 (continued)

Test Tube Number	Internal Pressure Test Results (bars)	ASME Section X Results (bars)	ASME Section X Failure Layer
E2 G1 A5 - 1	17	50-55	all layers
E2 G1 A5 - 2	10		
E2 G2 A5 - 4	17	40-45	all layers
E2 G2 A5 - 5	22		

The results obtained from ASME Boiler and Pressure Vessel Code, Section X are rather consistent with the experimental burst pressure test results, except being slightly lower. This is an expected result remembering that there lies an elastomeric internal liner inside the tubes. The liner also carries load during the experiments, but it is not shown in laminate analysis. Exploring the results, it was observed that for carbon fiber reinforced tubes manufactured with $[\pm 54°]_3$ $[90°]_1$ winding angle configuration, the laminate analysis give lower burst pressure data compared with the experimental results. The reason is that, the laminate analysis mentions that the failure starts from the outermost layer. According to the analysis, when a ply fails, the structure is accepted to be failed and the code gives the first ply failure pressure as the tube's failure pressure. However, in reality, the structure is still capable of carrying load, as observed in the experiment. During the experiment, the failure of the outermost layer can be followed from the stress – strain data of the tube as a change in slope, but the failure stress is much higher. Therefore, the higher burst pressure value observed at the experiment is reasonable. For both fiber types, the analysis results for [90°] winding angle configuration are higher than those of the experimental results, which probably is due to the extremely low strength of the winding configuration in axial direction, as discussed in the previous chapters. Failure modes for the glass fiber reinforced tubes are consistent with the failure modes deduced from their stress – strain data. Except the tubes of [90°] winding angle configuration, ASME Boiler and Pressure Vessel Code claims all the failures

to originate at the inner layers, which is the case in the tests, and can be verified by the changes in the slopes of the experimental stress – strain curves. The catastrophic failure cannot be differentiated from the failures that originate at the inner layers and for the carbon fiber reinforced tubes, it was concluded that experiments reveal no significant difference for the failure mode, as the stress – strain data are linear until failure. This suggested that all the layers might have failed instantly, that is, the failure is catastrophic, which would conflict the analysis results. But as mentioned before, another possibility is that the time interval between a possible first ply failure and final failure is so short that the recording speed of the strain gauge data acquisition system was unable to detect that first ply failure. As a result, it can be said that the burst pressure data is consistent with the laminate analysis.

CHAPTER VI

CONCLUSION AND RECOMMENDATIONS

The aim of the study was to to determine the mechanical characteristics of the filament wound composite tubes working under internal pressure loads, by experimentally measuring the mechanical properties like strains in hoop direction, maximum hoop stresses that are formed during internal pressure loading. Doing that, it was intended to identify and generate the necessary data to be used in the design applications and path a way to a new research on life assessment with health monitoring.

In order to determine the composite behavior, a total number of 52 internal pressure tests are applied on the composite tubes that are manufactured with wet filament winding method. The test are carried out according to ASTM D 1599-99 standard. Two different fiber types (glass and carbon fibers), two different fiber tension settings (default fiber tensioning and extra fiber tensioning) and five different winding angles (25°, 45°, 54°, 65° and 90°, with a single layer of hoop reinforcement on each) are employed in manufacturing of the tubes. The changes in internal pressure and the burst pressure are recorded. The strain data of each tube are obtained by strain gauges, and are evaluated with the stress data. Accordingly, the mechanical properties of the tubes are summarized in Table 6.1 and Table 6.2 for carbon and glass fiber reinforced tubes, respectively.

Table 6.1 Mechanical properties of carbon fiber reinforced tubes.

Winding Angle Configuration [±°][90°]	**Burst Pressure (bars)**	**Hoop Elastic Constant (GPa)**
25	78 - 159	17.4 - 22.3
45	418 - 422	47.2 - 54.7
54	498 - 540	98.3 - 120.3
65	134-141	166.3 - 299.4
90	17 - 26	25.3 - 39.5

Table 6.2 Mechanical properties of glass fiber reinforced tubes.

Winding Angle Configuration [±°][90°]	**Burst Pressure (bars)**	**Hoop Elastic Constant (GPa)**
25	91 - 236	17.8 - 37.8
45	274 -285	19.8 - 41.4
54	425 - 471	39 - 86
65	108 - 120	78.2 - 154.7
90	10 - 22	64 - 135.3

Evaluating the data, it was observed that carbon fiber reinforced tubes of $[\pm 54°]_3[90°]_1$ winding configuration shows the maximum burst performance. In general evaluation, the carbon fiber reinforced tubes exhibited better performance than glass fiber reinforced tubes. Also, $[\pm 54°][90°]_1$ winding configuration is the best performance for both fiber types. It was observed that burst pressure and hoop elastic constants are extensively dependent on the fiber type and winding angle configuration, but the effect of extra tensioning of fibers is insignificant on burst performance.

The burst pressure results are verified with the laminate analysis. “ASME Boiler and Pressure Vessel Code, Section X: Fiber-Reinforced Plastic Pressure Vessels” is employed in the laminate analysis. It was found that the burst pressure values and the failure modes offered by the analysis are rather consistent with the experimental results. The only significant difference in the results are for [90°] winding angle configuration, and the reason is decided to be the extreme weakness of the configuration in axial direction, which, resulted in the failure of the tube at very low pressure values. It was observed that internal pressure testing is a reliable method in determining the burst properties of filament wound structures.

In literature, internal pressure testing is commonly employed for the determination of mechanical properties. The factor that differentiates this study from the similar ones is that the tests in literature are applied to the composite tubes of lower wall thicknesses, whereas rather larger wall thicknesses are employed in this work. Filament winding operation significantly alters the microstructure and physical properties for low thicknesses. Very low wall thicknesses may result in the failure of the structure at the matrix regions, and thus, for successful simulation of the tests, wall thicknesses must be above a certain value. Another point is that, this work is almost able to simulate a pressure vessel, as there is a liner inside the structure, wall thicknesses are fairly large, and free – end condition is accomplished at the tests.

Studying with the composites, it should always be remembered that the properties of composites are not homogeneous throughout the structure. Their performance is highly dependent on the fabrication processes and parameters, and they are very sensitive to environmental conditions, storage and handling. Any defect or flaw that is possibly introduced during these stages can easily degrade the mechanical properties of the composites. This fact is once more verified by this work, as it was observed that the tubes that even belonged to the same parent tube can reveal very different performances. Due to this fact, it should again be emphasized that the composite materials shall require very large safety factors in design applications.

The evaluation of the strains and the determination of the strain value where the first failure is observed is very important for life assessment. For example, fatigue tests are generally carried out at some predefined stress values, which are the fractions of the strength of the material. The strain response of the composite to a certain value of stress obviously influences its fatigue life. If the formed strain in a material is large for constant stress, structure will deform easily and quicker, and thus the fatigue life will be shorter. Therefore, for the design applications that consider fatigue life, it is vital to know the strain response of the composite.

Another important aspect of the prediction of strain response of the composite may be that, the critical applications in which the geometric tolerances are very low, require low strains. High expansions and deformations are not permitted in those practices. Excessive expansions of such parts in a system may result in the degradation of the system properties of the overall structure. For design applications that require low geometric tolerances, having a knowledge about the strain response of the material is essential and crucial.

Considering the fatigue properties, a future study may be suggested as the determination of the fatigue life of filament wound composite tubes. Internal pressure fatigue life tests are carried out at certain predefined stress values, which are the fractions of the burst pressure of the material. Studying the burst pressures of the filament wound composite tubes that are manufactured with different production parameters in this work, a further step may be suggested as fatigue life determination of such structures by internal pressure testing.

The study considered the effects of the fiber type, winding angle configuration and extra tensioning of fibers on mechanical properties, but, it should be recalled that these variables are not the only production parameters of the filament winding process which affect the performance of the filament wound structures. Resin bath temperature, tex value of fibers, types of resin, winding patterns, winding ply configurations, hybridization, curing conditions and surface treatment may also

influence the properties of filament wound structures. For filament winding process optimization, a study that investigates the effect of these variables on mechanical properties can be suggested as another future work.

REFERENCES

[1] S.K. Mazumdar, *Composites Manufacturing: Materials, Product, and Process Engineering,* CRC Press, 2002.

[2] T. E. Miller, *Introduction to Composites*, Composites Institute Publications, 1990.

[3] J.W. Weeton, D.M. Peters, K.L. Thomas, *Engineers' Guide to Composite Materials,* ASM Publications, 1990.

[4] *ASTM D 3878-98 Standard Terminology for Composite Materials*, ASTM Standard, 1998.

[5] N. L. Hancox, R. M. Mayer, *Design Data For Reinforced Plastics*, Chapman & Hall, 1994.

[6] *Carbon and High Performance Fibers, Directory and Databook, Edition 6*, Chapman & Hall, 1995.

[7] M. M. Schwartz, *Composite Materials, Volume II: Processing, Fabrication, and Applications*, Prentice Hall Publications, 1997.

[8] *ASTM D 2290-04 Standard Test Method for Apparent Hoop Tensile Strength of Plastic or Reinforced Plastic Pipe by Split Disk Method,* ASTM Standard, 2004.

[9] *ASTM D 1599-99 Standard Test Method for Resistance to Short-Time Hydraulic Pressure of Plastic Pipe, Tubing, and Fittings*, ASTM Standard, 1999.

[10] *ASTM D 2143-00 Standard Test Method for Cyclic Pressure Strength of Reinforced, Thermosetting Plastic Pipe,* ASTM Standard, 2000.

[11] *ASTM D 2992-01 Standard Practice for Obtaining Hydrostatic or Pressure Design Basis for Fiberglass (Glass-Fiber-Reinforced Thermosetting-Resin) Pipe and Fittings,* ASTM Standard, 2001.

[12] *ASTM D 2105-01 Standard Test Method for Longitudinal Tensile Properties of Fiberglass (Glass-Fiber-Reinforced Thermosetting-Resin) Pipe and Tube,* ASTM Standard, 2001.

[13] *ASTM F 948-94(2001)e1 Standard Test Method for Time-to-Failure of Plastic Piping Systems and Components Under Constant Internal Pressure With Flow,* ASTM Standard, 2001.

[14] *ASTM D 3410/D3410M-03 Standard Test Method for Compressive Properties of Polymer Matrix Composite Materials with Unsupported Gage Section by Shear Loading*, ASTM Standard, 2003.

[15] *ASTM D 3479/D3479M-96(2002)e1 Standard Test Method for Tension-Tension Fatigue of Polymer Matrix Composite Materials*, ASTM Standard, 2002.

[16] *ASTM D 3518/D3518M-94(2001) Standard Test Method for In-Plane Shear Response of Polymer Matrix Composite Materials by Tensile Test of a ± 45^o Laminate*, ASTM Standard, 2001.

[17] P. Mertiny, F. Ellyin, and A. Hothan, *An Experimental Investigation on the Effect of Multi-Angle Filament Winding on the Strength of Tubular Composite Structures,* Composites Science and Technology, Vol 64, pp. 1-9, 2004

[18] P.D. Soden, R. Kitching, P.C. Tse, Y. Tsavalas, *Influence of Winding Angle on the Strength and Deformation of Filament Wound Composite Tubes Subjected to Uniaxial and Biaxial Loads,* Composites Science and Technology, Vol 46, pp. 363-378, 1992.

[19] P.D. Soden, R. Kitching, P.C. Tse, *Experimental Failure Stresses for ±55° Filament Wound Glass Fiber Reinforced Plastic Tubes Under Biaxial Loads*, Composites, Vol 20, Number 2, pp 125-134, 1989

[20] F. Ellyin, M. Carroll, D. Kujawski and A.S. Chiu, *The Behavior of Multidirectional Filament Wound Fibreglass/Epoxy Tubulars Under Biaxial Loading,* Composites Part A: Applied Science and Manufacturing, Vol 28, pp 781-790, 1997

[21] N.Tarakçioğlu, L.Gemi and A.Yapıcı, *Fatigue Failure Behavior of Glass/Epoxy ±55° Filament Wound Pipes Under Internal Pressure*, Composite Science and Technology, Vol 65, pp. 703-708, 2004

[22] A.S. Kaddour, M.J. Hinton, P.D. Soden, *Behaviour of ±45° Glass/Epoxy Filament Wound Tubes Under Quasi-Static Biaxial Tension – Compression Loading: Experimental Results,* Composites Part B: Engineering, Vol 34, pp. 689-704, 2003

[23] F. Ellyin and M. Martens, *Biaxial Fatigue Behaviour of a Multidirectional Filament-Wound Glass-Fiber/Epoxy Pipe*, Composites Science and Technology, Vol 61, pp 491-502, 2001

[24] C. Kaynak, O. Mat, *Uniaxial Fatigue Behavior of Filament Wound Glass-Fiber/Epoxy Composite Tubes,* Composites Science and Technology, Vol 61, pp. 1833-1840, 2001

[25] J. Bai, P. Seeleuthner, and P. Bompard, *Mechanical Behavior of ±55° Filament-Wound Glass-Fibre/Epoxy-Resin Tubes: I. Microstructural Analyses, Mechanical Behavior and Damage Mechanisms of Composite Tubes Under Pure Tensile Loading, Pure Internal Pressure, and Combined Loading,* Composites Science and Technology, Vol 57, pp 141-153, 1997

[26] M.R. Etemad, E. Pask and C.B. Besant, *Hoop Strength Characterization of High Strength Carbon Fibre Composites,* Composites, Vol 23, pp 253-259, 1992

[27] L. Parnas and N. Katırcı, *Design of Fiber-Reinforced Composite Pressure Vessels Under Various Loading Conditions*, Composite Structures, Vol 58, pp. 83-95, 2002

[28] P.M. Wild and G.W. Vickers, *Analysis of Filament-Wound Cylindrical Shells Under Combined Centrifugal, Pressure and Axial Loading,* Composites Part A, Vol 28A, pp. 47-55, 1997

[29] J.-S Park, C.-S. Hong, C.-G. Kim and C.-U. Kim, *Analysis of Filament Wound Composite Structures Considering the Change of Winding Angles Through the Thickness Direction,* Composite Structures, Vol 55, pp 63-71, , 2002

[30] C. Gargiulo, M. Marchetti, and A. Rizzo, *Prediction of Failure Envelopes of Composite Tubes Subjected to Biaxial Loadings*, Acta Astronautica, Vol 39, pp 355-368, 1996

[31] M. Xia, K. Kemmochi and H. Takayanagi, *Analysis of Filament-Wound Fiber-Reinforced Sandwich Pipe Under Combined Internal Pressure and Thermomechanical Loading,* Composite Structures, Vol 51, pp 273-283, 2001

[32] X.-K. Sun, S.-Y. Du, and G.-D Wang, *Bursting Problem of Filament Wound Composite Pressure Vessels,* International Journal of Pressure Vessels and Piping, Vol 76, pp 55-59, 1999

[33] A. S. Kaddour, M. J. Hinton and P. D. Soden, *Behaviour of ±45° Glass/Epoxy Filament Wound Composite Tubes Under Quasi-Static Equal Biaxial Tension–Compression Loading: Experimental Results,* Composites Part B: Engineering, Vol 34, pp 689-704, 2003